arxiv:1401.7274

On Yangian-invariant regularisation of deformed on-shell diagrams in $\mathcal{N} = 4$ super-Yang–Mills theory

Niklas Beisert, Johannes Broedel and Matteo Rosso

Institut für Theoretische Physik,
Eidgenössische Technische Hochschule Zürich
Wolfgang-Pauli-Strasse 27, 8093 Zürich, Switzerland

{nbeisert,jbroedel,mrosso}@itp.phys.ethz.ch

arXiv:1401.7274v2 [hep-th] 26 Aug 2014

Abstract

We investigate Yangian invariance of deformed on-shell diagrams with $D = 4$, $\mathcal{N} = 4$ superconformal symmetry. We find that invariance implies a direct relationship between the deformation parameters and the permutation associated to the on-shell graph. We analyse the connection with deformations of scattering amplitudes in $\mathcal{N} = 4$ super-Yang–Mills theory and the possibility of using the deformation parameters as a regulator preserving Yangian invariance. A study of higher-point tree and loop graphs suggests that manifest Yangian invariance of the amplitude requires trivial deformation parameters.

Contents

1 Introduction **2**

2 Yangian invariance **3**
2.1 Yangian symmetry and representation on spinor variables 3
2.2 Yangian invariants from undeformed building blocks 5
2.3 Yangian invariants from deformed building blocks 7
2.4 Deformed on-shell graphs and the permutation flow 9
2.5 Superconformal and Yangian Anomalies 14

3 On-shell graphs and scattering amplitudes **15**
3.1 Grassmannian formalism 15
3.2 Top-cell vs. BCFW decomposition, deformation and compatibility 17
3.3 Deformation of the six-point NMHV amplitude 19
3.4 The central charge as a regulator for the four-point one-loop amplitude . . 21
3.5 Discussion 25

4 Conclusions **26**

A Yangian invariance of deformed glued objects **26**

B Grassmannian integrals from on-shell graphs **28**

C One-loop integral singular support **30**

---

1 Introduction

One of the most striking features of the $\mathcal{N} = 4$ super-Yang–Mills (sYM) theory is that its tree-level S-matrix is invariant under the infinite-dimensional Yangian algebra $\mathrm{Y}[\mathfrak{psu}(2,2|4)]$ [1], see also [2, 3]. This symmetry arises as the closure of the ordinary superconformal symmetry together with the hidden dual superconformal symmetry the theory possesses [4]. The existence of this infinite-dimensional symmetry algebra is another important evidence in support of the conjectured integrability of the planar sector of the theory, see [5]. It is however well known that IR divergences break the (dual) superconformal symmetry of scattering amplitudes at loop level to some extent [4].

In ref. [6], the authors proposed an interesting construction relating Yangian invariants in $\mathcal{N} = 4$ sYM to so-called on-shell graphs (or on-shell diagram). These graphs are associated with integrals over suitably defined subspaces of Grassmannian manifolds and provide a direct link to the Grassmannian formulation of scattering amplitudes, introduced and studied in refs. [7–10].

In refs. [11], the authors introduced *deformed* on-shell graphs, where the deformation consists of the shift of the helicities of the external legs by a complex value. In this article we focus on the conditions for manifest Yangian invariance for such deformed graphs.

A topic which is worth investigating in this framework is the relation between deformed on-shell diagrams and scattering amplitudes, a relation which is currently unclear. We will

study the possibility of constructing such a correspondence in the context of the tree-level Britto–Cachazo–Feng–Witten (BCFW) recursion relations and their supersymmetric extension [12]. Our starting point will be the formulation of the BCFW recursion relations in terms of undeformed on-shell graphs. We will subsequently focus on one simple example, the six-point NMHV amplitude, and study the possibility of constructing a manifestly Yangian-invariant deformed amplitude as a sum of deformed Yangian invariants.

In refs. [11] it was also proposed that the deformation parameters could be used as regulators for loop amplitudes. As an example, the four-point one-loop amplitude in $\mathcal{N} = 4$ sYM was explicitly computed for a particular choice of deformation which happens to break Yangian invariance. We will address the question of the compatibility of this regulating method with Yangian invariance by computing the four-point one-loop deformed on-shell graph with a Yangian-preserving set of deformation parameters.

The paper is organised as follows: In sec. 2 we review the concept of Yangian invariance, we define undeformed and deformed on-shell graphs and discuss the conditions these deformed on-shell graphs have to satisfy in order to be Yangian invariant. Section 3 deals with the translation from Yangian invariants represented by deformed on-shell graphs to scattering amplitudes. We will focus in particular on tree-level NMHV amplitudes as well as the four-point one-loop amplitude in $\mathcal{N} = 4$ sYM and discuss their compatibility with the deformation of external helicities. Section 4 contains a summary of the results.

2 Yangian invariance

A mechanism to build Yangian invariants starting from three-point vertices in $\mathcal{N} = 4$ sYM and producing so-called on-shell diagrams was developed in ref. [6]. Yangian invariance, however, allows for more general building blocks: in this chapter we will use *deformed* three-point vertices (developed in ref. [11]) and investigate the properties of the resulting deformed on-shell diagrams. The relation to scattering amplitudes in $\mathcal{N} = 4$ sYM theory will be discussed in sec. 3 below.

2.1 Yangian symmetry and representation on spinor variables

The Yangian algebra $\mathrm{Y} := \mathrm{Y}[\mathfrak{g}]$ is a quantum algebra based on (half of) the affine extension of the Lie algebra[1] $\mathfrak{g}$. In addition to the generators $\mathfrak{J}^a$ of the Lie algebra $\mathfrak{g}$ obeying the usual Lie-algebra relations

$$[\mathfrak{J}^a, \mathfrak{J}^b] = f_c^{ab}\, \mathfrak{J}^c, \tag{2.1}$$

there are level-one generators $\widehat{\mathfrak{J}}^a$ satisfying

$$[\mathfrak{J}^a, \widehat{\mathfrak{J}}^b] = f_c^{ab}\, \widehat{\mathfrak{J}}^c\,, \tag{2.2}$$

and the Serre relations

$$\Big[\big[\mathfrak{J}^a, \widehat{\mathfrak{J}}^b\big], \widehat{\mathfrak{J}}^c\Big] + \Big[\big[\mathfrak{J}^b, \widehat{\mathfrak{J}}^c\big], \widehat{\mathfrak{J}}^a\Big] + \Big[\big[\mathfrak{J}^c, \widehat{\mathfrak{J}}^a\big], \widehat{\mathfrak{J}}^b\Big] = f_d^{ag} f_e^{bh} f_f^{ci} f_{ghi}\, \mathfrak{J}^{\{d} \mathfrak{J}^e \mathfrak{J}^{f\}}\,, \tag{2.3}$$

[1] In what follows, we will not distinguish between Lie algebras and Lie superalgebras. When considering Lie superalgebras, all expressions should be understood with the appropriate graded symmetrisation and factors of $(-1)^{\deg(\dots)}$.

where $\{\ldots\}$ means graded symmetrisation of indices. The complete Yangian algebra $\mathrm{Y}[\mathfrak{g}]$ is obtained by successively commuting level-zero and level-one generators. The coproduct $\Delta : \mathrm{Y} \to \mathrm{Y}\otimes\mathrm{Y}$ of the Yangian algebra is defined on the level-zero and level-one generators as

$$\Delta(\mathfrak{J}^a) := \mathfrak{J}^a \otimes 1 + 1 \otimes \mathfrak{J}^a \quad \text{and} \quad \Delta(\widehat{\mathfrak{J}}^a) := \widehat{\mathfrak{J}}^a \otimes 1 + 1 \otimes \widehat{\mathfrak{J}}^a + f^a_{bc}\, \mathfrak{J}^b \otimes \mathfrak{J}^c, \tag{2.4}$$

respectively.

In this article, we will consider $\mathrm{Y}[\mathfrak{psu}(2,2|4)]$, the Yangian of the maximal superconformal algebra in four dimensions. A convenient representation of $\mathfrak{psu}(2,2|4)$ acts on functions defined on the on-shell superspace with spinor-helicity variables $\lambda^\alpha, \tilde\lambda^{\dot\alpha}$ and Grassmann variables $\tilde\eta^A$. Here, dotted and undotted Greek spinor indices take the values 1 and 2, and capital Latin indices correspond to a four-dimensional fundamental representation of SU(4).

The spinors λ and $\tilde\lambda$ are related to the massless momentum vector via $p_\mu = \sigma_{\mu\,\alpha\dot\alpha}\lambda^\alpha\tilde\lambda^{\dot\alpha}$, where $\sigma_{\mu\alpha\dot\alpha}$ are generalised Pauli matrices which have to be chosen according to the spacetime signature. Here we work with complexified momenta, which amounts to treating λ and $\tilde\lambda$ as independent complex variables [13]. For a fixed external momentum p_μ the spinors λ and $\tilde\lambda$ are defined up to a rescaling

$$\lambda \to \alpha\lambda, \qquad \tilde\lambda \to \alpha^{-1}\tilde\lambda\,, \tag{2.5}$$

where α is an arbitrary nonzero complex number. In the supersymmetric part of the on-shell space, the Grassmann variables have to scale as

$$\tilde\eta \to \alpha^{-1}\tilde\eta \tag{2.6}$$

for consistency. Imposing reality of momenta in signature $(1,3)$ amounts to equating $\tilde\lambda = \pm\bar\lambda$, where the sign depends on the sign of the energy. This implies that the freedom of rescaling $\lambda, \tilde\lambda$ for real momenta is restricted to multiplication by a phase.

In this representation, the generators of $\mathfrak{psu}(2,2|4)$ read (see ref. [14])

$$\begin{aligned}
\mathfrak{L}^\alpha_{\ \beta} &= \lambda^\alpha\frac{\partial}{\partial\lambda^\beta} - \tfrac{1}{2}\delta^\alpha_{\ \beta}\lambda^\gamma\frac{\partial}{\partial\lambda^\gamma}, & \bar{\mathfrak{L}}^{\dot\alpha}_{\ \dot\beta} &= \lambda^{\dot\alpha}\frac{\partial}{\partial\lambda^{\dot\beta}} - \tfrac{1}{2}\delta^{\dot\alpha}_{\ \dot\beta}\lambda^\gamma\frac{\partial}{\partial\lambda^\gamma},\\
\mathfrak{Q}^{A\alpha} &= \lambda^\alpha\tilde\eta^A, & \bar{\mathfrak{Q}}^{\dot\alpha}_A &= \tilde\lambda^{\dot\alpha}\frac{\partial}{\partial\tilde\eta^A},\\
\mathfrak{S}_{A\alpha} &= \frac{\partial^2}{\partial\lambda^\alpha\partial\tilde\eta^A}, & \bar{\mathfrak{S}}^A_{\dot\alpha} &= \tilde\eta^A\frac{\partial}{\partial\tilde\lambda^{\dot\alpha}},\\
\mathfrak{R}^A_{\ B} &= \tilde\eta^A\frac{\partial}{\partial\tilde\eta^B} - \tfrac{1}{4}\delta^A_B\tilde\eta^C\frac{\partial}{\partial\tilde\eta^C}, & \mathfrak{D} &= \tfrac{1}{2}\lambda^\gamma\frac{\partial}{\partial\lambda^\gamma} + \tfrac{1}{2}\tilde\lambda^{\dot\gamma}\frac{\partial}{\partial\tilde\lambda^{\dot\gamma}} + 1,\\
\mathfrak{P}^{\alpha\dot\alpha} &= \lambda^\alpha\tilde\lambda^{\dot\alpha}, & \mathfrak{K}_{\alpha\dot\alpha} &= \frac{\partial^2}{\partial\lambda^\alpha\partial\tilde\lambda^{\dot\alpha}}.
\end{aligned} \tag{2.7}$$

The above representation of the Lie superalgebra $\mathfrak{psu}(2,2|4)$ can be lifted to an evaluation representation of the Yangian $\mathrm{Y}[\mathfrak{psu}(2,2|4)]$, for which the level-one generators act as $\widehat{\mathfrak{J}} \simeq u\mathfrak{J}$. Here u is called the evaluation parameter of the representation. In the evaluation representation, the left-hand-side of the Serre relation eq. (2.3), reduces to the usual Jacobi identity. Accordingly, the right hand side can be shown to vanish.

With the evaluation representation on disposal, one can construct the action of the Yangian algebra on functions depending on several variables in the on-shell superspace.

This action can be obtained from the maximally iterated coproduct

$$\Delta^{n-1}(\widehat{\mathfrak{J}}^a) = \sum_{k=1}^{n} \widehat{\mathfrak{J}}^a_k + f^a_{bc} \sum_{1\leq i<j\leq n} \mathfrak{J}^b_i \, \mathfrak{J}^c_j = \sum_{k=1}^{n} u_k \mathfrak{J}^a_k + f^a_{bc} \sum_{1\leq i<j\leq n} \mathfrak{J}^b_i \, \mathfrak{J}^c_j, \tag{2.8}$$

where the first equality holds due to the definition of the coproduct eq. (2.4), whereas the second equality applies to evaluation representations. The evaluation parameters u_k can (and will) be different for each element of the tensor product.

In addition to the generators defined in eq. (2.7) there is another important quantity for the discussion to follow: the central charge operator $\mathfrak{C}$ that appears in the anticommutator of $\mathfrak{Q}, \mathfrak{S}$

$$\big\{\mathfrak{Q}^{A\alpha}, \mathfrak{S}_{B\beta}\big\} = \delta^A_B \mathfrak{L}^\alpha_\beta - \delta^\alpha_\beta \mathfrak{R}^A_B + \tfrac{1}{2}\delta^A_B \delta^\alpha_\beta \big[\mathfrak{D} + \tfrac{1}{2}\mathfrak{C}\big]. \tag{2.9}$$

It is represented by

$$\mathfrak{C} := \lambda^\alpha \frac{\partial}{\partial \lambda^\alpha} - \tilde{\lambda}^{\dot\alpha} \frac{\partial}{\partial \tilde{\lambda}^{\dot\alpha}} - \tilde{\eta}^A \frac{\partial}{\partial \tilde{\eta}^A} + 2\,. \tag{2.10}$$

In the algebra $\mathfrak{psu}(2,2|4)$, the central charge operator $\mathfrak{C}$ is set to zero. If one however considers the central extension to $\mathfrak{su}(2,2|4)$, the operator $\mathfrak{C}$ does not need to vanish any more.

A function $\mathcal{Y}(\{\lambda_i, \tilde{\lambda}_i, \tilde{\eta}_i\})$, $i = 1, \ldots, n$ is called a Yangian invariant if it is annihilated by the maximally iterated coproduct $\Delta^{n-1}(\ldots)$ for all operators $\mathfrak{J}$ and $\hat{\mathfrak{J}}$. In particular, for the charge operator the condition reads

$$\sum_{i=1}^{n} \mathfrak{C}_i \, \mathcal{Y}(\{\lambda_i, \tilde{\lambda}_i, \tilde{\eta}_i\}) = 0. \tag{2.11}$$

One can understand the eigenvalue of the operator $\mathfrak{C}_i$ as an additional scaling weight for the i-th copy of the superspace the Yangian invariant is defined upon. In particular the variable λ_i now scales with a factor $\alpha^{(1+c_i)}$. With nonzero c_i one is effectively working on a weighted projective space.

2.2 Yangian invariants from undeformed building blocks

Yangian-invariant objects for constructing scattering amplitudes in $\mathcal{N} = 4$ sYM theory have been explored in ref. [6] in order to derive an all-loop generalisation of the BCFW recursion relations [12].

The main tool in the investigation of Yangian invariants in ref. [6] are undeformed on-shell graphs, which are planar graphs obtained by gluing two types of basic Yangian-invariant building blocks. The building blocks used are the MHV and $\overline{\text{MHV}}$ three-point tree-level superamplitudes in $\mathcal{N} = 4$ sYM theory.

After reviewing the undeformed formalism in the current subsection, we are going to study deformed building blocks and check under which circumstances the corresponding deformed on-shell graphs are Yangian invariants.

Undeformed vertices Expressed in spinor-helicity and Grassmann variables of the on-shell superspace introduced in subsec. 2.1, the two basic building blocks used in ref. [6] read

$$\mathcal{A}_{3,\text{MHV}} = \frac{\delta^4(P)\,\delta^8(Q)}{\langle 12\rangle\langle 23\rangle\langle 31\rangle}, \qquad \mathcal{A}_{3,\overline{\text{MHV}}} = \frac{\delta^4(P)\,\delta^4(\tilde{Q})}{[12][23][31]}, \tag{2.12}$$

where $P^{\alpha\dot{\alpha}} := \sum_{i=1}^{3} \lambda_i^{\alpha} \tilde{\lambda}_i^{\dot{\alpha}}$ is the total four-momentum, whereas $Q^{A\alpha} := \sum_{i=1}^{3} \lambda_i^{\alpha} \tilde{\eta}_i^{A}$ and $\tilde{Q}^{A} := [12]\tilde{\eta}_3^{A} + [23]\tilde{\eta}_1^{A} + [31]\tilde{\eta}_2^{A}$. Furthermore, $\langle ij \rangle = \lambda_i^{\alpha} \lambda_{j\alpha}$ and $[ij] = \tilde{\lambda}_{i\dot{\alpha}} \tilde{\lambda}_j^{\dot{\alpha}}$, where indices are raised and lowered with dotted and undotted totally antisymmetric 2×2 tensors ϵ, where $\epsilon_{12} = \epsilon_{\dot{1}\dot{2}} = -1$.

Being superamplitudes in $\mathcal{N} = 4$ sYM theory, these two three-vertices are Yangian invariants, as shown for example in refs. [1, 3]. However, for now we would like to focus on their symmetries without making reference to their amplitude properties.

We will represent $\mathcal{A}_{3,\mathrm{MHV}}$ and $\mathcal{A}_{3,\overline{\mathrm{MHV}}}$ with a black and a white dot, respectively,

. (2.13)

Undeformed on-shell graphs In this paragraph we briefly review the formalism of on-shell graphs (or diagrams). In particular we will address how to build higher-point Yangian invariants by gluing the basic building blocks introduced in eq. (2.12).

Let us consider two trivalent graphs for simplicity. If we consider their product with one leg identified,

$$\mathcal{F}_5(p_1, p_2, p_3, p_4, p_I) := \mathcal{A}_{3,\mathrm{MHV}}(p_1, p_2, p_I)\, \mathcal{A}_{3,\overline{\mathrm{MHV}}}(-p_I, p_3, p_4), \tag{2.14}$$

then it is not clear how to treat the state corresponding with momentum p_I. Explicitly, if we consider I as an external state, then the total momentum is $\sum_{i=1}^{4} \mathfrak{P}_i^{\alpha\dot{\alpha}} + \mathfrak{P}_I^{\alpha\dot{\alpha}}$, which clearly does not annihilate $\mathcal{F}_5$. On the other hand, if we consider the external states to be just $1, 2, 3$ and 4, the total momentum is $\sum_{i=1}^{4} \mathfrak{P}_i^{\alpha\dot{\alpha}}$ and it does annihilate $\mathcal{F}_5$, but now p_I acts as a "preferred" momentum that breaks Lorentz invariance[2]. Therefore, the mere identification of a leg between two superconformal invariants does not give another superconformal invariant.

In order to render the combination of $\mathcal{A}_{3,\mathrm{MHV}}(p_1, p_2, p_I)$ and $\mathcal{A}_{3,\overline{\mathrm{MHV}}}(-p_I, p_3, p_4)$ a superconformal invariant, one has to integrate over the on-shell superspace corresponding to the identified leg with the measure

$$\int \frac{\mathrm{d}^2\lambda_I\, \mathrm{d}^2\tilde{\lambda}_I}{\mathrm{Vol}[\mathrm{GL}(1)]}\, \mathrm{d}^4\tilde{\eta}_I, \tag{2.15}$$

a procedure which we will call *gluing*.

Invariance under the total momentum generator $\mathfrak{P}^{\alpha\dot{\alpha}} = \sum_{i=1}^{4} \mathfrak{P}_i^{\alpha\dot{\alpha}}$ is ensured by the overall delta $\delta(\sum_{i=1}^{4} p_i)$. The resulting glued object can be checked to be invariant under superconformal as well as dual superconformal transformations provided the building blocks are Yangian invariants, as shown in ref. [9].

Correspondingly, one can introduce a graphical description of Yangian invariants in terms of so-called *on-shell graphs*: connected planar graphs constructed by gluing trivalent black and white vertices associated to $\mathcal{A}_{3,\mathrm{MHV}}$ ($\mathcal{A}_{3,\overline{\mathrm{MHV}}}$) as in eq. (2.13) and where each internal line corresponds to an integration over the on-shell phase space. For example, eq. (2.16) represents the graph obtained by gluing together $\mathcal{A}_{3,\mathrm{MHV}}$ and $\mathcal{A}_{3,\overline{\mathrm{MHV}}}$

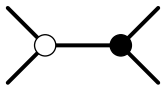

. (2.16)

[2]It can be seen as follows: the spinor products *are* Lorentz invariant (since the delta functions allow us to substitute $p_I = p_1 + p_2$), but a Lorentz transformation acting only on $1, 2, 3, 4$ does not leave the delta functions invariant.

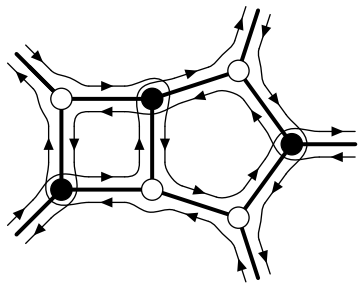

Figure 1: Permutation flow associated with a 5-point graph.

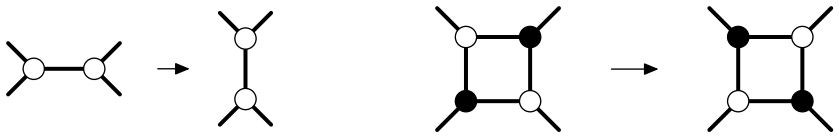

Figure 2: Merger and square move

In ref. [6] it was shown how the equivalence of different on-shell graphs can be encoded in a purely combinatorial object: the *permutation* σ associated with the on-shell graph. If two on-shell graphs represent the same Yangian invariant, they will encode the same permutation. The permutation associated with an on-shell graph is a bijective map

$$\sigma : \{1, \ldots, n\} \to \{1, \ldots, n\} \ , \tag{2.17}$$

which is constructed as follows: starting from an external point i of an on-shell graph, follow the internal lines turning right at each black vertex and left at each white vertex. The image $\sigma(i)$ is given by the ending external line j. In fig. 1 there is an example for the permutation obtained from following the rules described above.

The equivalence of two on-shell graphs can be deduced graphically. There are two graphical transformations that do not affect the permutation: *merging* and *square move*. Merging changes the way four lines are connected by two equally coloured vertices, while the square move rotates a subgraph consisting of a square of vertices with alternating colours by 90°. Both operations are depicted in fig. 2.

2.3 Yangian invariants from deformed building blocks

Deformed vertices The undeformed building blocks $\mathcal{A}_{3,\mathrm{MHV}}$ and $\mathcal{A}_{3,\overline{\mathrm{MHV}}}$ defined in eq. (2.12) do not only satisfy the central-charge condition for Yangian invariance eq. (2.11), but the stronger constraint

$$\mathfrak{C}_i \cdot \mathcal{A}_{3,\mathrm{MHV}} = 0, \qquad \mathfrak{C}_i \cdot \mathcal{A}_{3,\overline{\mathrm{MHV}}} = 0, \tag{2.18}$$

that is, the operator $\mathfrak{C}$ defined in eq. (2.10) vanishes for each component of the tensor product individually. Taking into account the gluing procedure above, it is not difficult to see that this statement generalises to all Yangian invariants represented by undeformed on-shell graphs

$$\mathfrak{C}_i \, \mathcal{Y} = 0 \tag{2.19}$$

for all i. Following the analysis of ref. [11], we will exploit the fact that the condition for Yangian invariance eq. (2.11) is less restrictive than eq. (2.19). In particular, we will start with *deformed* trivalent objects $\mathcal{A}_\bullet$ and $\mathcal{A}_\circ$, which are not annihilated by the central

charge operators $\mathfrak{C}_i$ individually as in eq. (2.19). After discussing under which conditions these deformed building blocks are Yangian invariants, we will explore in which way one can combine the deformed building blocks in order to obtain new Yangian invariants.

The deformation of the building blocks $\mathcal{A}_\bullet$ and $\mathcal{A}_\circ$ will be naturally given in terms of nonzero eigenvalues c_i corresponding to each operator $\mathfrak{C}_i$. The eigenvalue c_i is referred to as the *central charge* and is accompanied by an evaluation parameter u_i (see subsec. 2.1) for each component i of the tensor product. As stated at the end of subsec. 2.1, in this configuration the parameters u_k of the evaluation representation of the Yangian need not be all equal.

In general, we consider the central charge to be ingoing for all external particles. However, for each internal line one has to choose a direction for the flow of central charge. Graphically, this is represented by an arrow, whose reversal amounts to flipping the central charge flowing along the line while keeping the evaluation parameter untouched:

(2.20)

It can be seen as follows: considering the line to be a 2-point invariant, the action of the level-zero generators must satisfy

$$\mathfrak{J}_1 + \mathfrak{J}_2 = 0, \tag{2.21}$$

which (for $\mathfrak{J} = \mathfrak{C}$) implies $c_1 = -c_2$. For the level one, we have

$$\widehat{\mathfrak{J}}_1 + \widehat{\mathfrak{J}}_2 = u_1\,\mathfrak{J}_1 + u_2\,\mathfrak{J}_2 = (u_1 - u_2)\,\mathfrak{J}_1 = 0, \tag{2.22}$$

meaning that $u_1 = u_2$.

For the objects $\mathcal{A}_\bullet$ and $\mathcal{A}_\circ$ we choose the following convention:

(2.23)

which corresponds to

$$\mathfrak{C}_i\,\mathcal{A}_\bullet = c_i \mathcal{A}_\bullet, \qquad \mathfrak{C}_i\,\mathcal{A}_\circ = c_i \mathcal{A}_\circ. \tag{2.24}$$

The condition for Yangian invariance eq. (2.11) requires the total central charge operator to annihilate the vertex

$$\sum_{i=1}^{3} \mathfrak{C}_i \cdot \mathcal{A}_\bullet = 0, \qquad \sum_{i=1}^{3} \mathfrak{C}_i \cdot \mathcal{A}_\circ = 0, \tag{2.25}$$

which translates into the condition $c_1 + c_2 + c_3 = 0$ immediately. In [11], two building blocks $\mathcal{A}_\bullet$ and $\mathcal{A}_\circ$ satisfying the condition eq. (2.24) have been introduced. Represented in spinor-helicity variables, they read

$$\mathcal{A}_\bullet = \frac{\delta^4(P)\delta^8(Q)}{\langle 12\rangle^{1+c_3}\langle 23\rangle^{1+c_1}\langle 31\rangle^{1+c_2}}, \qquad \mathcal{A}_\circ = \frac{\delta^4(P)\delta^4(\tilde{Q})}{[12]^{1-c_3}[23]^{1-c_1}[31]^{1-c_2}}\,. \tag{2.26}$$

While it is not difficult to check the invariance of $\mathcal{A}_\bullet$ and $\mathcal{A}_\circ$ under the superconformal generators eq. (2.7), Yangian invariance is ensured only after imposing vanishing under one level-one generator $\widehat{\mathfrak{J}}$. We choose to consider the action of the operator $\widehat{\mathfrak{P}}^{\alpha\dot{\alpha}}$ on $\mathcal{A}_\bullet$, $\mathcal{A}_\circ$

in order to derive a relation between the central charges[3] c_i and the evaluation parameters u_i, which is a necessary condition for Yangian invariance.

The level-one operator $\widehat{\mathfrak{P}}^{\alpha\dot\alpha}$ can be derived from eq. (2.8) and reads

$$\widehat{\mathfrak{P}}^{\alpha\dot\alpha} = \sum_{1\le i<j\le n} \Big[\big(\delta^{\dot\alpha}_{\dot\beta}\mathfrak{L}^{\alpha}_{i\,\beta} + \delta^{\alpha}_{\beta}\bar{\mathfrak{L}}^{\dot\alpha}_{i\,\dot\beta} + \delta^{\dot\alpha}_{\dot\beta}\delta^{\alpha}_{\beta}\mathfrak{D}_i\big)\mathfrak{P}_j^{\beta\dot\beta} + \bar{\mathfrak{Q}}^{\dot\alpha}_{iA}\mathfrak{Q}_j^{A\alpha} - (i\leftrightarrow j)\Big] + \sum_{k=1}^{n} u_k \mathfrak{P}_k^{\alpha\dot\alpha}\,. \tag{2.27}$$

The action of $\widehat{\mathfrak{P}}$ on $\mathcal{A}_\bullet$ is easily computed, as the terms in square brackets in eq. (2.27) are all single-derivative operators. Then, a short calculation leads to

$$\widehat{\mathfrak{P}}^{\alpha\dot\alpha}\cdot\mathcal{A}_\bullet = \Big\{ \big[c_2+c_3+u_1\big]\lambda_1^\alpha\tilde\lambda_1^{\dot\alpha} + \big[c_3-c_1+u_2\big]\lambda_2^\alpha\tilde\lambda_2^{\dot\alpha} + \big[-c_1-c_2+u_3\big]\lambda_3^\alpha\tilde\lambda_3^{\dot\alpha}\Big\}\mathcal{A}_\bullet. \tag{2.28}$$

A similar equation can be derived for $\mathcal{A}_\circ$, the only difference being the sign with which the central charges appear. Since the p_k's sum to zero, there are just two independent equations, and the solution expressing the c's in terms of the evaluation parameters reads after imposing $c_1+c_2+c_3=0$

$$\mathcal{A}_\bullet: \qquad c_1 = u_2-u_3, \quad c_2 = u_3-u_1, \quad c_3 = u_1-u_2\,; \tag{2.29}$$

$$\mathcal{A}_\circ: \qquad c_1 = u_3-u_2, \quad c_2 = u_1-u_3, \quad c_3 = u_2-u_1\,. \tag{2.30}$$

Notice that shifting all the u's by a common quantity α has the only effect of sending $\widehat{\mathfrak{P}} \to \widehat{\mathfrak{P}} + \alpha\,\mathfrak{P}$, and this shift does not affect eq. (2.27). Therefore, the evaluation parameters u_i are defined up to an overall shift.

This type of analysis – albeit in the language of another set of variables and for a limited set of on-shell graphs – was first done in ref. [11].

2.4 Deformed on-shell graphs and the permutation flow

Having introduced the deformed building blocks $\mathcal{A}_\bullet$ and $\mathcal{A}_\circ$ in eq. (2.26), let us now discuss how to glue them in order to obtain Yangian invariants. In parallel to the previous discussion, a deformed on-shell graph is a connected planar graph composed by gluing the deformed building blocks.

In contrast to the gluing procedure for the undeformed graphs built from undeformed blocks eq. (2.12), we will have to take care of the central charge c and the evaluation parameter u associated to each internal and external line. Gluing two vertices with a common leg I is again done by integrating over the on-shell superspace corresponding to this particular leg using the measure eq. (2.15). The combined object is a Yangian invariant with the following assignment for the internal central charge c_I and evaluation parameter u_I

$$\int \frac{\mathrm{d}^2\lambda_I\,\mathrm{d}^2\tilde\lambda_I}{\mathrm{Vol}[\mathrm{GL}(1)]}\,\mathrm{d}^4\tilde\eta_I \mathcal{A}_\bullet\big(\lambda_I,\tilde\lambda_I,\tilde\eta_I,c_I,u_I\big)\,\mathcal{A}_\circ\big(\lambda_I,-\tilde\lambda_I,-\tilde\eta_I,-c_I,u_I\big), \tag{2.31}$$

where we omitted the dependence on the on-shell superspace variables of particles $1,2,3,4$ in the integrand. In app. A it is shown that the identifications of c_I and u_I in eq. (2.31) ensure the Yangian invariance of the resulting object.

[3] Our naming conventions differ from those used by the authors of ref. [11]; the "spectral parameters" of these references are called central charges here.

An object represented by a deformed on-shell graph is a Yangian invariant if the central charges and evaluation parameters on each internal line are identified as described above and eqs. (2.29), (2.30) are satisfied at each vertex. Imposing all those constraints simultaneously leads to a system of linear equations relating the central charges c_i and evaluations parameters u_i of the external legs.

Two equally coloured vertices Let us see how this works for an easy example: imposing all constraints for the graph

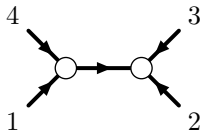

(2.32)

leads to

$$\begin{aligned} 0 &= c_1 + c_2 + c_3 + c_4, \\ u_2 &= c_1 + c_2 + u_1, \\ u_3 &= c_1 + 2c_2 + c_3 + u_1, \\ u_4 &= c_2 + c_3 + u_1. \end{aligned} \tag{2.33}$$

It is not difficult to see that the solution to the above system could have been obtained from another set of linear equations, corresponding to the following graph:

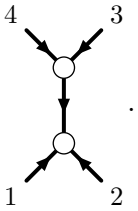

. (2.34)

This does not come unexpectedly: the merger operation is valid for deformed on-shell graphs as well, as already shown in ref. [11].

Chain of vertices Let us now look at another trivial configuration: a tree on-shell graph with n external legs, $n_{\mathrm{V}} = n - 2$ vertices and $n_{\mathrm{I}} = n - 3$ internal lines, for example

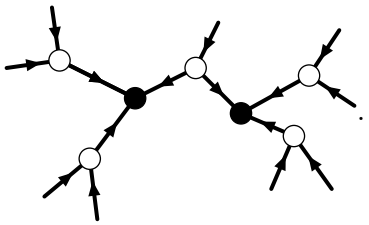

. (2.35)

As discussed in subsec. 2.3, there are three free parameters associated to each vertex. This turns the consideration of a tree graph into an easy problem: taking the two conditions for gluing an internal line into account a simple counting shows that the number of independent quantities for the Yangian invariant in eq. (2.35) equals the number n of external lines:

$$n = 3\, n_{\mathrm{V}} - 2\, n_{\mathrm{I}}\,. \tag{2.36}$$

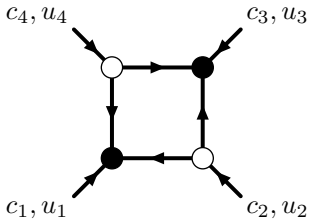

Figure 3: Four-point on-shell graph

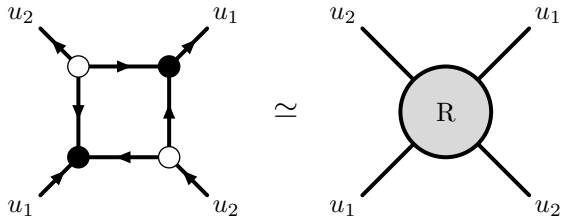

Figure 4: The four-point tree-level deformed on-shell graph has a structure resembling the R-matrix $\mathrm{R}(u_1 - u_2)$ of quantum integrable systems. Note that in order to match the usual conventions for R-matrices, we have reversed the arrows of the four-point on-shell diagram with respect to fig. 3.

Four-point graph, four vertices In order to produce more interesting configurations, one will need to build on-shell diagrams containing loops. Let us have a look at the simplest case: a box with alternating white and black dots depicted in fig. 3.

Solving the linear system corresponding to the four-point on-shell graph in fig. 3 leads to

$$c_1 = -c_3, \quad c_2 = -c_4 \quad \text{and} \quad u_1 = u_3, \quad u_2 = u_4\,. \tag{2.37}$$

Thus the values of the evaluation parameters and central charges can be identified between legs 1 and 3 as well as legs 2 and 4 respectively. Note furthermore that the condition in eq. (2.11) is trivially satisfied with the above solution.

The construction and study of this four-point deformed on-shell graph was performed in ref. [11], where it was argued that it intertwines the external states. In quantum integrable systems, this is the rôle played by the R-matrix, see fig. 4. It depends on the difference of the evaluation parameters of the external states, which is a natural fact in the context of quantum integrable systems.

Let us then explore the properties of R-matrices in quantum integrable systems a little closer before translating their properties back to the language of on-shell diagrams. Note that all the following equations featuring on-shell graphs are to be understood as "the linear system for the graph on the right-hand side is equivalent to the linear system represented on the left-hand side".

- R-matrices satisfy the Yang–Baxter equation:

$$\mathrm{R}_{12}(u_1-u_2)\mathrm{R}_{13}(u_1-u_3)\mathrm{R}_{23}(u_2-u_3) = \mathrm{R}_{23}(u_2-u_3)\mathrm{R}_{13}(u_1-u_3)\mathrm{R}_{12}(u_1-u_2) \tag{2.38}$$

  or in terms of R-matrix and on-shell diagrams:

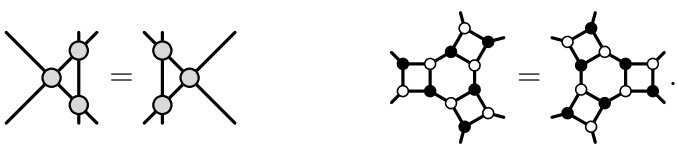

(2.39)

- Iterated application is proportional to the identity

$$\mathrm{R}_{12}(u_1-u_2)\mathrm{R}_{21}(u_2-u_1) = f(u_1,u_2)\cdot I \qquad \sim \quad , \quad \sim \quad , \tag{2.40}$$

where the function $f(u_1, u_2)$ is some function of the two spectral parameters.

After identifying the four-point Yangian invariant in fig. 3 with $\mathrm{R}(u_1 - u_2)$, it is worthwhile to investigate the diagram further. In particular, one can define new variables

$$u^{\pm} = u \pm c\,, \tag{2.41}$$

which are convenient for tracking how central charges c_i and evaluation parameters u_i flow through on-shell diagrams. The quantity u^+ will be written to the left of a line looking in the direction of its arrow, while u^- will be placed to the right. This convention is compatible with flipping the direction of the arrow using the rules in subsec. 2.3

$$\overset{u^+}{\underset{u^-}{\longrightarrow}} \quad . \tag{2.42}$$

After solving the linear system one finds the configuration in fig. 5. Tracing the quantities $u^{\pm}$ through the diagram and connecting them by lines, one can easily recognise the following rules for traversing:

- at a black vertex, turn right,
- at a white vertex, turn left.

Thus it is suggestive to keep track of this information in terms of the following double-line formalism. Hereby the black and white vertices translate into

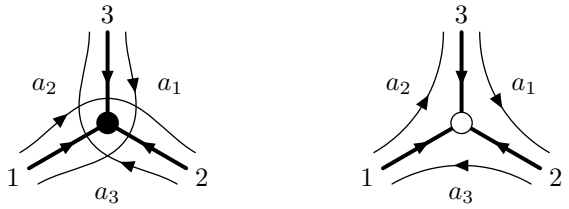

(2.43)

and fig. 5 becomes fig. 6, where we did not draw the vertices and their connecting lines for convenience. Comparing the above rules with the definition of the permutation represented by an on-shell graph introduced in subsec. 2.2, it becomes obvious that the quantities $u^{\pm}$ follow exactly the lines determining the permutations. In other words, the permutation map σ defined in eq. (2.17) above keeps track of the flow of the $u^{\pm}$ between external legs. The two vertices defined above are sufficient to translate any on-shell graph into the linear system of equations ensuring Yangian invariance immediately, as will be shown below.

The four-point diagram discussed here is the subgraph appearing in the square-move transformation of the undeformed on-shell graph depicted in fig. 2. Employing the double-line formalism, it is trivial to see that his transformation does not alter the permutation in the deformed setup either: switching the rôle of black and white vertices amounts to switching the path a quantity takes around the loop (see fig. 6), while the solution to the conditions ensuring Yangian invariance remains unchanged.

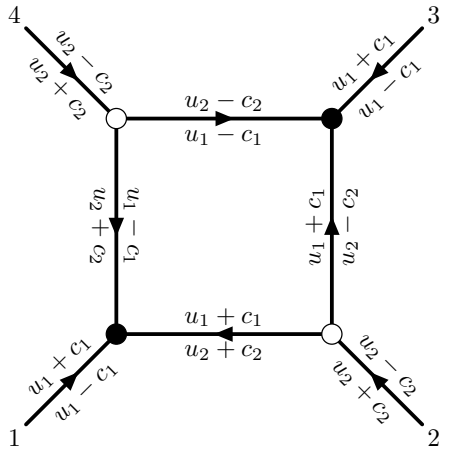

Figure 5: Four-point on-shell graph with flows of $u^{\pm}$ indicated

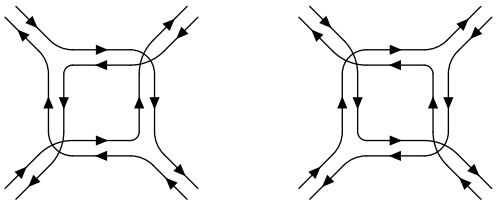

Figure 6: Four-point on-shell graph in the double-line formalism and its square-moved version. The square simply switches the rôle of the flow: a line going around the loop clockwise will do so counterclockwise after the square move.

Five points and seven vertices In order to check the identification between the flow of $u^{\pm}$ and the permutation encoded in an on-shell graph, let us consider another example: the five-point on-shell diagram

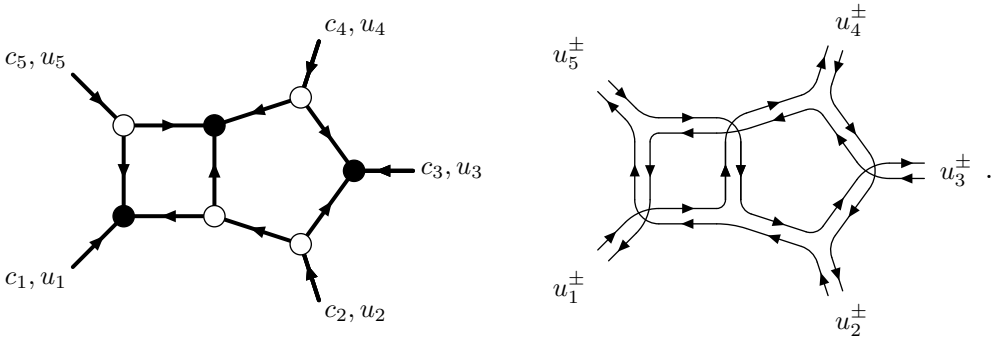

(2.44)

Imposing Yangian invariance by solving the linear system yields

$$\{u_1^+, u_2^+, u_3^+, u_4^+, u_5^+\} = \{u_4^-, u_5^-, u_1^-, u_2^-, u_3^-\}\,, \tag{2.45}$$

which corresponds to the permutation $(1,2,3,4,5) \to (4,5,1,2,3)$ – a simple cyclic shift by three.

The same result is implied by the second diagram in the above picture. With the double-line formalism it is obvious that the linear system obtained by imposing Yangian invariance of the corresponding on-shell diagram will fix at most half of the $2n$ free variables c_i and u_i, $i = 1 \ldots n$. The solution to the linear system can be expressed in the permutation σ defined in subsec. 2.2. Considering all external particles as ingoing, the solution simply reads

$$u_{\sigma(i)}^- = u_i^+\,. \tag{2.46}$$

2.5 Superconformal and Yangian Anomalies

In this subsection we would like to comment on the issue of exactness of Yangian invariance and on the uniqueness of the invariants we have constructed.

A common belief in integrable systems is that the extended symmetries present in such systems determine the observables uniquely. In particular, the S-matrix should be determined uniquely by its invariance.

In the previous parts of this section we have constructed a large collection of Yangian invariants which are – most likely – almost all inequivalent. Here it makes sense to compare only those functions with the same external data (number of legs, MHV degree, central charges and evaluation parameters).

It is quite clear that for a given set of external data there exist several on-shell graphs: At a low number of loops in the on-shell diagram, there will only be few, if any, graphs whose permutation structure matches the external data. However, at higher on-shell loops, there must be further graphs with the same permutation structure because the set of permutation structures for a given number of legs is finite. It is unlikely that all of these graphs reproduce the same function, in particular as they are not all connected by the permissible merger and square moves (see fig. 2).

This argument seems to show that there are many inequivalent Yangian invariants for the same external data. However, following the analysis in ref. [15] (see ref. [16] for a review), the flaw of the argument is that the derived functions are not actually Yangian *invariant*. The reason is that the fundamental three-point functions spoil superconformal and Yangian symmetry in a subtle way. They are invariant for almost all external *momentum* configurations, but invariance breaks down when all three momenta are exactly collinear.[4] This can be observed most easily in the following form of the three-point vertex (2.26)

$$\begin{aligned} A_\bullet = \operatorname{sign}\big(\langle 12\rangle\big) \int \frac{d\tilde{z}_1}{\tilde{z}_1^{1+c_1}} \frac{d\tilde{z}_2}{\tilde{z}_2^{1+c_2}} \, \delta^2(\tilde{z}_1\lambda_1 + \tilde{z}_2\lambda_2 + \lambda_3) \\ \cdot \delta^2(\tilde{\lambda}_1 - \tilde{z}_1\tilde{\lambda}_3)\, \delta^2(\tilde{\lambda}_2 - \tilde{z}_2\tilde{\lambda}_3)\, \delta^4(\tilde{\eta}_1 - \tilde{z}_1\tilde{\eta}_3)\, \delta^4(\tilde{\eta}_2 - \tilde{z}_2\tilde{\eta}_3). \end{aligned} \tag{2.47}$$

The sign factor multiplying the integral is responsible for conformal "anomaly" at collinear momenta $\delta A_\bullet = \delta \operatorname{sign}\big(\langle 12\rangle\big) \cdot \ldots$. In particular, the deformations in the weights w.r.t. $\tilde{z}_1$ and $\tilde{z}_2$ do not interfere with the symmetry breaking.

The anomaly of an on-shell graph is the sum of the anomalies of all constituent vertices.[5]

δ 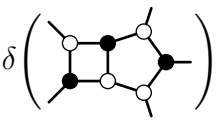 $=$ $\sum_{\text{vertices}}$ 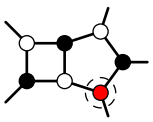 . (2.48)

This form demonstrates that the overall anomaly depends on the precise structure of the on-shell graph. Two inequivalent graphs with equal external structure have a different anomaly structure, and therefore they are expected to have a different functional dependence. This is most evident if the graphs have a different number of on-shell loops. Moreover one may wonder whether the merger and square moves are in fact *exact* equivalences of graphs in the above sense.

[4] The discussion requires a real signature of spacetime. It is most straight-forward in $(2,2)$ split signature where three-point function actually exist, therefore let us assume this signature.

[5] This is the behaviour for $(2,2)$ split signature. For $(3,1)$ Minkowski signature the anomaly works differently, and requires a suitable combination of contributions to the S-matrix, see ref. [17] for further comments.

3 On-shell graphs and scattering amplitudes

In the preceding section we developed the tools to construct deformed Yangian invariants. In the following section, we want to investigate whether it is possible and meaningful to introduce deformed scattering amplitudes as (sums of) deformed on-shell graphs preserving manifest Yangian invariance.

We start with a short review of the formalism linking undeformed on-shell graphs with ordinary scattering amplitudes; the interested reader can find the complete formalism in ref. [6] and references therein. We then investigate the possibility to deform tree-level amplitudes using deformed Yangian-invariant on-shell graphs. Finally, following the spirit of [11], we investigate whether it is possible to use the deformation parameters as Yangian-preserving regulators for the four-point one-loop amplitude of $\mathcal{N} = 4$ sYM. We discuss our findings at the end of the section.

3.1 Grassmannian formalism

In this subsection we briefly review the Grassmannian formulation of scattering amplitudes in $\mathcal{N} = 4$ sYM – first introduced in ref. [7] – and its relation to on-shell graphs, which has been developed in ref. [6]. The discussion assumes familiarity with the BCFW recursion relations and its supersymmetric extension [12] as well as the concepts of helicity amplitudes.

Grassmannian manifolds The *Grassmannian manifold* $G(k, n)$ (from now on simply "Grassmannian") is the space of complex k-planes in $\mathbb{C}^n$ passing through the origin. It is a generalisation of the notion of complex projective space; in particular, $\mathbb{CP}^{n-1}$ is the Grassmannian manifold $G(1, n)$. A k-plane in $\mathbb{C}^n$ is uniquely determined by a set of k linearly independent complex n-tuples, therefore one can identify a point in $G(k, n)$ with an equivalence class of $k \times n$ complex matrices C of rank k. In fact, given such a matrix C, the right action of $\mathrm{GL}(k)$ maps C to a different matrix C'. Since C and C' identify the same k-plane in $\mathbb{C}^n$, we can identify the Grassmannian $G(k, n)$ with the space of $k \times n$ rank-k complex matrices modulo a $\mathrm{GL}(k)$ rescaling. The matrix represents the k n-vectors that identify the plane in $\mathbb{C}^n$.

Let us introduce two further notions used in the Grassmannian language: a *top-cell* of the above chart of the Grassmannian $G(k, n)$ is the cell where all sets of k consecutive columns of the matrix C become linearly independent. Its dimension is the full dimension $k(n - k)$ of $G(k, n)$. On the contrary, a *generic* cell is allowed to have sets of linearly dependent consecutive columns in its matrix C. The *stratification* of the Grassmannian is then defined to be the system of nested boundaries of cells, where a boundary is described by the above linearly dependent configuration of columns. The decomposition of cells depends on the choice of coordinates on the Grassmannian $G(k, n)$.

Scattering amplitudes as integrals over Grassmannians The authors of refs. [7,6] showed that it is possible to express tree-level as well as loop amplitudes in $\mathcal{N} = 4$ sYM as integrals over Grassmannian manifolds. In particular, the tree-level amplitude can be

written as the following integral

$$\mathcal{A}_{k,n} := \int \frac{\mathrm{d}^{k\times n}C_{ra}}{\mathrm{Vol}[\mathrm{GL}(k)]} \frac{1}{(12\ldots k)(23\ldots k+1)\ldots(n-1\ldots k-1)} \prod_{r=1}^{k} \delta^{4|4}\Big(\sum_{a=1}^{n} C_{ra}\,\mathcal{Z}_a\Big), \tag{3.1}$$

where $(i\ldots i+k)$ is the i-th k-minor of the matrix C and $\mathcal{Z} = (\lambda, \mu; \tilde{\eta})$ are supertwistor variables, as introduced in [14]. Most of the integrations in eq. (3.1) are fixed by the bosonic delta functions; the number of bosonic integrals left to be evaluated via contour integration is $(k-2)(n-k-2)$. Notice that eq. (3.1) makes superconformal symmetry manifest, since supertwistor variables $\mathcal{Z}$ transform linearly under PSU$(2,2|4)$.

In order to proceed to loop amplitudes it is useful to introduce yet another way of expressing on-shell graphs. In ref. [6] it was shown that any on-shell graph with n_{F} faces can be associated with an integral of an $(n_{\mathrm{F}}-1)$-form defined on the Grassmannian $G(k,n)$, where the parameters k and n are related to the on-shell graph via

$$k = n_{\mathrm{w}} + 2\,n_{\mathrm{b}} - n_{\mathrm{i}} \qquad \text{and} \qquad n = 3\,(n_{\mathrm{b}} + n_{\mathrm{w}}) - 2\,n_{\mathrm{i}}\ . \tag{3.2}$$

Here, n_{w} denotes the number of white vertices, n_{b} the number of black vertices and n_{i} the number of internal lines.

Each on-shell graph can be associated with a matrix C denoting a cell of the Grassmannian, which in turn is a function of $n_{\mathrm{F}}-1$ auxiliary *face variables* f_i. Expressed in these face variables, the integral associated with the on-shell graph is obtained by integrating over all internal lines and takes the form

$$\prod \frac{\mathrm{d}f_i}{f_i}\,. \tag{3.3}$$

Accordingly, amplitudes are constructed by supplementing the measure eq. (3.3) with the appropriate delta functions coming from the gluing of three-vertices. This leads to the integral

$$\mathcal{I}_{\text{graph}} = \int \Big[\prod_{i=1}^{n_{\mathrm{F}}-1} \frac{\mathrm{d}f_i}{f_i}\Big]\, \delta^{2k}\Big(\sum_{a=1}^{n} C_{ra}(f_i)\tilde{\lambda}_a\Big)\, \delta^{2(n-k)}\Big(\sum_{s=1}^{n-k} C_{sa}(f_i)\lambda_s\Big)\, \delta^{0|4k}\Big(\sum_{a=1}^{n} C_{ra}(f_i)\tilde{\eta}_a\Big). \tag{3.4}$$

The above integral is a generalisation of eq. (3.1), which in addition allows to describe loop amplitudes. The precise connection between undeformed on-shell graphs and (loop) amplitudes is nontrivial. We do not discuss the relation between face variables and the matrix C representing a point in the Grassmannian here. The interested reader may consult ref. [6] for the complete formalism, or ref. [11] for a concise review in the light of the deformations introduced in the following sections.

All-loop BCFW recursion relations in the Grassmannian formalism In ref. [6] it was pointed out that the BCFW recursion relations in the Grassmannian formalism are obtained as solutions to a formal boundary equation. This equation states that the singularities of an amplitude in $\mathcal{N} = 4$ sYM theory are given solely by factorisation channels and forward limits, where

- a factorisation channel refers to the splitting of an amplitude in the special kinematical situation where the sum of consecutive momenta becomes on-shell;

- a forward limit of an on-shell l-loop amplitude is an $(l-1)$-loop amplitude with two additional legs with opposite momentum. We refer to ref. [18] for the analysis of the rôle played by forward limits in the description of loop amplitudes.

The solution to this formal boundary equation is a sum of on-shell diagrams, each of which corresponds to a BCFW channel. In particular, the solution provides the integrand for the associated scattering amplitude[6]. Since each summand is a Yangian invariant, this proves that the integrand for any loop amplitude in $\mathcal{N}=4$ sYM theory is a Yangian invariant modulo partial integration [8]. However, loop amplitudes in $\mathcal{N}=4$ sYM theory do not exhibit Yangian invariance, as dealing with IR divergences breaks conformal invariance.

Conveniently, the on-shell graphs representing the BCFW channels for a tree-level amplitude $\mathcal{A}_{n,k}$ can as well be expressed as boundaries of the top-cell[7] of a certain codimension. The boundaries of a cell are obtained graphically by removing specific edges (called *removable edges* in ref. [6]) from the associated on-shell graph.

The identification of the boundaries of the cell associated with a given on-shell graph together with the BCFW construction allows to express any tree-level amplitude starting from the top-cell.

For loop amplitudes there is no analogue of a top-cell object, that is, an on-shell graph whose boundaries directly yield the BCFW channels.

3.2 Top-cell vs. BCFW decomposition, deformation and compatibility

In the following subsection we will investigate the possibility of linking deformed on-shell graphs with "deformed" amplitudes in $\mathcal{N}=4$ sYM. In order to do so, we will first review the tools developed in ref. [11] that relate a Grassmannian integral to a deformed on-shell graph. Subsequently we will turn to the interplay between on-shell graphs, BCFW decomposition and Yangian invariance.

Grassmannian integral for deformed scattering amplitudes The integral corresponding to a deformed on-shell graph is obtained by deforming the ordinary measure eq. (3.3). In terms of the face variables f_i, the deformation reads

$$\prod_{i=1}^{n_{\mathrm{F}}} \frac{\mathrm{d}f_i}{f_i} \;\to\; \prod_{i=1}^{n_{\mathrm{F}}} \frac{\mathrm{d}f_i}{f_i^{1+\zeta_i}}\,. \tag{3.5}$$

Here the *face shifts* ζ are dual variables with respect to the central charge c; the latter is obtained from the difference of the two adjacent face shifts[8]

$$\zeta_a - \zeta_b = c \tag{3.6}$$

[6]Upon dimensional regularisation, additional terms breaking dual conformal invariance can appear [19]. These terms are not present in the purely four-dimensional analysis such as the one-loop amplitude considered below.

[7]It is possible to show (see ref. [20]) that an on-shell graph representing the top-cell for a certain k and n corresponds to a permutation which is just a cyclic shift by k. Furthermore, in the aforementioned paper it was explained how to construct a representative on-shell graph for the top-cell.

[8]For a three-point vertex this identity makes the c's have the same relationship to the u's as to the ζ's. Therefore, the ζ's must agree locally with the u's up to an overall shift. Note that the latter shift depends on the position and hence the ζ's are not equivalent to the u's.

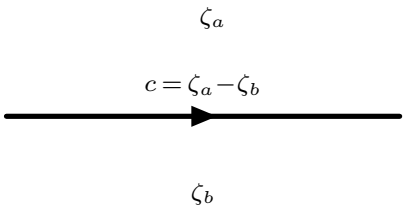

Figure 7: Face variables and central charges

as depicted in fig. 7. It is evident that the resulting deformed integrand is not a meromorphic function any more. This is an important fact, since it questions a clear interpretation of the BCFW decomposition of the deformed amplitudes.

Deformed scattering amplitudes In the context of $\mathcal{N} = 4$ sYM theory, it makes sense to try to construct Yangian-invariant deformed scattering amplitudes. Naturally, those deformed amplitudes should not violate unitarity, that is, they should have the correct singularity structures. In the undeformed case, this is ensured via the BCFW construction. As pointed out in the previous subsection, the BCFW recursion relations simultaneously maintain Yangian invariance.

In order to define a deformed Yangian-invariant amplitude there are two natural approaches:

- One could start from the collection of on-shell diagrams corresponding to the undeformed BCFW channels. One would need to deform those in a Yangian-invariant way individually and subsequently demand compatibility between the deformations, meaning that the parameters u_i and c_i attached to the external legs must be equal for all diagrams. The compatibility among the diagrams will lead to constrained configurations.

- One could deform the on-shell graphs corresponding to the top-cell. However, we have argued above that the integrand resulting from a deformed on-shell diagram is not meromorphic. In terms of the Grassmannian integral a boundary is equivalent to a pole given by the vanishing of a minor. Thus the nonmeromorphicity of the integrand associated with a deformed top-cell prevents a direct BCFW-like decomposition. It is however possible to constrain the deformation parameters in such a way that the removal of the edges corresponding to BCFW channels amounts to a simple residue integral.

For undeformed tree-level MHV amplitudes the BCFW decomposition of the amplitude consists of a single term and thus a single on-shell graph, which is the top-cell. The deformation of this on-shell graph directly translates into the deformation of the associated amplitude. For example, the on-shell graph depicted in fig. 5 corresponds to the deformed four-point tree-level amplitude.

For general tree-level amplitudes, these two procedures could in principle lead to different deformations of the amplitude, since in the second case it is not necessarily true that the resulting channels are Yangian invariant by themselves. Moreover, it could (and will) also happen that the only possible solution is the undeformed BCFW decomposition. In the following subsection we will study an easy example and analyse the results originating in the two approaches.

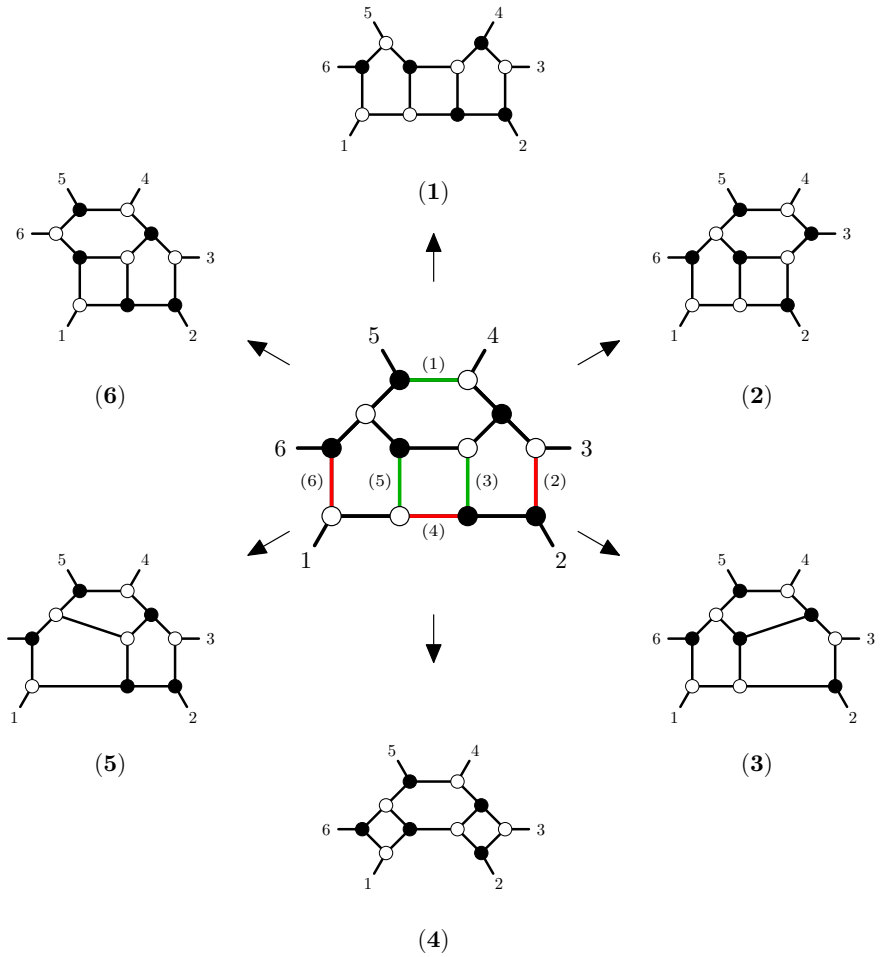

Figure 8: Codimension-one boundaries of the top-cell of $G(3,6)$; the removable edges are highlighted.

Considering general loop amplitudes, the definition of a top-cell–like object is not clear. Only in the case of the one-loop four-point amplitude there seems to be the analogue of a top-cell. We will investigate Yangian invariant deformations of this particular on-shell graph in subsec. 3.4 below.

3.3 Deformation of the six-point NMHV amplitude

Let us study the simplest nontrivial example: the six-point NMHV amplitude $\mathcal{A}_{6,3}$. The simplicity of this amplitude originates from the fact that the on-shell graphs representing the BCFW channels are codimension-one boundaries of the top-cell (as opposed to boundaries of higher codimension for other amplitudes). The top-cell graph associated with $G(3,6)$ and its six codimension-one boundaries are depicted in fig. 8. The two possible BCFW decompositions of $\mathcal{A}_{6,3}$ are given by adding either the contributions from graphs 1, 3 and 5 or 2, 4 and 6. In the following we will choose the latter one.

We will now investigate how to deform the on-shell graphs corresponding to $\mathcal{A}_{6,3}$ following the two different approaches described at the end of subsec. 3.2.

Deformation of the BCFW terms We will follow the first approach and impose Yangian invariance on the deformed on-shell graphs 2, 4 and 6 of fig. 8 separately, which

graph	permutation	$u \pm c$
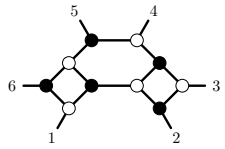	$\begin{matrix}1&2&3&4&5&6\\ \downarrow&\downarrow&\downarrow&\downarrow&\downarrow&\downarrow\\ 4&5&6&2&1&3\end{matrix}$	$u_1^+ = u_4^-,\quad u_2^+ = u_5^-,\quad u_3^+ = u_6^-,$ $u_4^+ = u_2^-,\quad u_5^+ = u_1^-,\quad u_6^+ = u_3^-,$
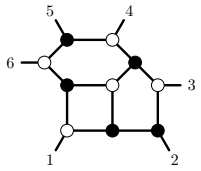	$\begin{matrix}1&2&3&4&5&6\\ \downarrow&\downarrow&\downarrow&\downarrow&\downarrow&\downarrow\\ 3&5&6&1&2&4\end{matrix}$	$u_1^+ = u_3^-,\quad u_2^+ = u_5^-,\quad u_3^+ = u_6^-,$ $u_4^+ = u_1^-,\quad u_5^+ = u_2^-,\quad u_6^+ = u_4^-,$
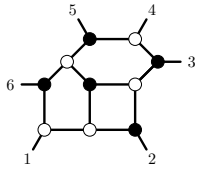	$\begin{matrix}1&2&3&4&5&6\\ \downarrow&\downarrow&\downarrow&\downarrow&\downarrow&\downarrow\\ 4&6&5&1&2&3\end{matrix}$	$u_1^+ = u_4^-,\quad u_2^+ = u_6^-,\quad u_3^+ = u_5^-,$ $u_4^+ = u_1^-,\quad u_5^+ = u_2^-,\quad u_6^+ = u_3^-.$

Figure 9: Permutation and parameter assignment for the BCFW decomposition of the six-point NMHV amplitude

amounts to satisfying the conditions implied by the double-line formalism introduced in subsec. 2.4.

For our choice of graphs, the permutations and their corresponding deformations are listed in fig. 9. Compatibility between the three channels is achieved by imposing all conditions simultaneously. Doing so, there are three remaining degrees of freedom: choosing $(u_3^+,\, u_5^+,\, u_6^+) := (a, b, c)$ as parameters, one finds

$$\begin{aligned}
&(u_1^+,\, u_1^-) = (c, b), && (u_2^+,\, u_2^-) = (a, b), && (u_3^+,\, u_3^-) = (a, c),\\
&(u_4^+,\, u_4^-) = (b, c), && (u_5^+,\, u_5^-) = (b, a), && (u_6^+,\, u_6^-) = (c, a).
\end{aligned} \tag{3.7}$$

We stress that the deformation described above is obtained by imposing Yangian invariance on each on-shell graph individually. We will see in the next paragraph how this result compares to the other approach.

Residues of the top-cell The boundaries of an undeformed on-shell graph can be obtained by removing a single edge from the graph. However, only specific internal edges can be removed consistently [6]. For the top-cell graph of $\mathcal{A}_{6,3}$, the removable edges are highlighted in fig. 8.

Taking a codimension-one boundary of a graph corresponds to calculating a residue of the Grassmannian integral. The lack of meromorphicity of the deformed integrand makes the task of taking the residue nontrivial, since one has to take care of the branch-cut structure. It is, however, always possible to force the integral associated with the removal of a removable edge to be meromorphic: the additional condition one has to impose is the vanishing of the central charge associated with that particular edge. A rigorous derivation of the sufficiency of this condition can be found in app. B.

Yangian invariance of the top-cell corresponds to the permutation and linear system reported in fig. 10. Enforcing the vanishing of central charges on all three edges to be

graph	permutation	$u \pm c$
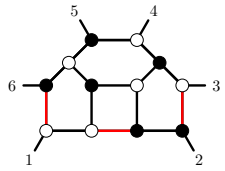	$\begin{matrix}1&2&3&4&5&6\\ \downarrow&\downarrow&\downarrow&\downarrow&\downarrow&\downarrow\\ 4&5&6&1&2&3\end{matrix}$	$u_1^+ = u_4^-,\quad u_2^+ = u_5^-,\quad u_3^+ = u_6^-,$ $u_4^+ = u_1^-,\quad u_5^+ = u_2^-,\quad u_6^+ = u_3^-.$

Figure 10: Permutation and parameter assignment for the top-cell on-shell graph for the six-point NMHV amplitude.

removed amounts to setting

$$u_5^+ = u_4^+ \,, \qquad u_2^+ = u_3^+ \,, \qquad u_1^+ = u_6^+ \,. \tag{3.8}$$

Consistently, the combination of the conditions reported in tab. 10 and in eq. (3.8) is equivalent to eq. (3.7).

It is possible to check that also the alternative BCFW decomposition – involving graphs 1, 3 and 5 of fig. 8, which corresponds to the removal of the green lines – admits a nontrivial deformation compatible with the codimension-one boundaries of the top-cell. Imposing vanishing of the central charges flowing on the red and green lines fig. 8 simultaneously leads to a linear system forcing all evaluation parameters to be equal and all central charges to be zero: Yangian invariance can only be realised in the undeformed case, as there are not enough degrees of freedom available.

The fact that the different on-shell graphs constituting a particular BCFW decomposition of a given tree-level NMHV amplitude admit a nontrivial common deformation is peculiar to the six-point case. Already for 7-point NMHV, imposing the compatibility for the deformations of the six on-shell graphs representing the six BCFW channels gives only the trivial solution: all central charges are forced to vanish and all evaluation parameters are equal. This is to be expected, since for tree amplitudes the number of BCFW channels for fixed k grows roughly quadratically with n, whereas the number of free deformation parameters is of order n.

Therefore – with the exception of MHV amplitudes and a few low-multiplicity examples in the non-MHV sector – it is not possible to express a deformed amplitude as a sum of deformed objects which are Yangian-invariant individually because the constraints arising from demanding compatibility between the Yangian-invariant constituent graphs lead to the trivial deformation: all central charges are fixed to zero and all spectral parameters are equal.

3.4 The central charge as a regulator for the four-point one-loop amplitude

In refs. [11] the possibility of using the deformation parameters as regulators for loop amplitudes was investigated. The authors considered and computed a deformed on-shell graph which – in the undeformed limit – corresponds to the four-point one-loop MHV amplitude. The result was manifestly finite, but it turned out not to preserve Yangian symmetry essentially because the latter was not taken into account in the construction.

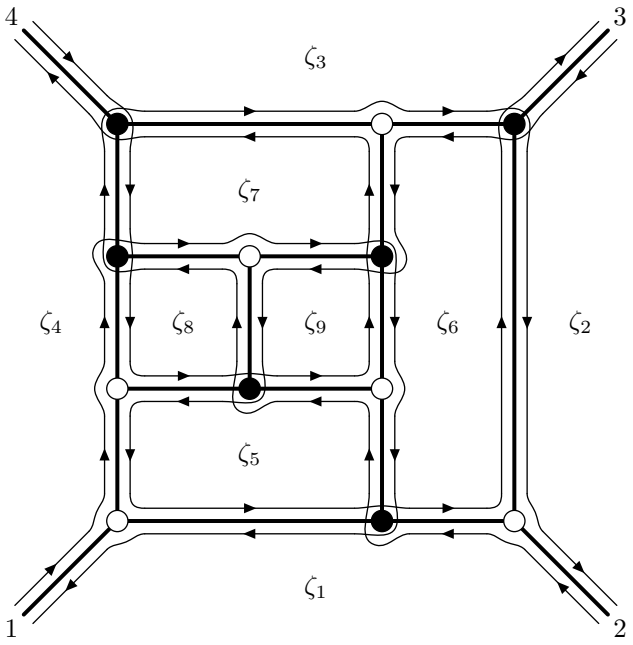

Figure 11: Four-point one-loop on-shell graph

Our focus is to investigate the possibility of using a Yangian-preserving deformation as a means to regulate loop amplitudes. The case of study will again be the on-shell graph that corresponds to the four-point one-loop MHV amplitude in the undeformed limit[9]. We evaluate the integral corresponding to a Yangian-invariant deformation and study its finiteness. As we shall see, the result we find is rather unexpected and curious.

The on-shell graph associated with the four-point one-loop amplitude is drawn in fig. 11, where we labelled the face shifts defined above eq. (3.6) by $\zeta_1 \dots \zeta_9$. Imposing Yangian invariance forces all external charges to vanish, which corresponds to the equality of all external face shifts $\zeta_1 \dots \zeta_4$. The face shifts are related to the evaluation parameters u_i of the external legs via

$$\begin{aligned} \zeta_1 = \zeta_2 = \zeta_3 = \zeta_4 = \Delta, \qquad & \zeta_5 = \Delta + u_3 - u_1, \\ \zeta_6 = \Delta + u_3 - u_2, \qquad & \zeta_7 = \Delta + u_4 - u_2, \\ \zeta_8 = \Delta + u_4 - u_1, \qquad & \zeta_9 = \Delta + u_4 - u_1 + u_3 - u_2, \end{aligned} \tag{3.9}$$

as can be easily obtained by following the parameters $u^{\pm}$ along the permutation lines in fig. 11. As already stated, this assignment of face shifts here preserves Yangian invariance and differs from the one studied in refs. [11].

The technique to construct the loop integral in terms of local variables was described by the authors of refs. [11]. As computed in these papers, the deformed four-point one-loop amplitude can be expressed in terms of a massless box integral with a deformed integrand, whose deformation is reminiscent of analytic regularisation:

$$\mathcal{A}_{4,2}^{\text{1-loop}}(\{a_i\}; s, t) = s\, t\, \mathcal{A}_{4,2}^{\text{tree}} \cdot I_{\text{box}}(\{a_i\}; s, t), \tag{3.10}$$

where $s = 2k_1 \cdot k_2$ and $t = 2k_2 \cdot k_3$ are Mandelstam variables and the deformed one-loop

[9]The impossibility of conciliating consistently BCFW decomposition and deformation of on-shell diagrams – investigated in subsec. 3.3 – does not pose any problem here, since in the undeformed limit this graph is the only graph corresponding to the four-point one-loop amplitude.

box integral reads[10]

$$I_{\text{box}}(\{a_i\};s,t) = \int \frac{\mathrm{d}^4 q}{(q^2)^{1+a_1}[(q+k_1)^2]^{1+a_2}[(q+k_1+k_2)^2]^{1+a_3}[(q-k_4)^2]^{1+a_4}}. \tag{3.11}$$

Here the variables a_i are the following combinations of the evaluation parameters u_k

$$a_1 = u_4 - u_1, \qquad a_2 = u_3 - u_4, \qquad a_3 = u_2 - u_3, \qquad a_4 = u_1 - u_2, \tag{3.12}$$

which implies $\delta := \sum_i a_i = 0$. However, for the following calculation it is advisable to keep the dependence on δ explicit, as it will provide easier access to the singular behaviour later on. Introducing Feynman parameters x_k, the integral can be rewritten as

$$\begin{aligned} I_{\text{box}} &= \frac{\Gamma(4+\sum_i a_i)}{\prod_{j=1}^4 \Gamma(1+a_j)} \int \mathrm{d}^4 q \int_0^1 \prod_{k=1}^4 \Big[\mathrm{d}x_k\, x_k^{a_k}\Big]\, \delta\Big(1 - \sum_{i=1}^4 x_i\Big) \times \\ &\qquad \times \Big[\Big(\sum_{i=1}^4 x_i\Big) q^2 + 2q\cdot(x_2 k_1 + x_3 k_1 + x_3 k_2 - x_4 k_4) + x_3\, s\Big]^{-4-\sum_{i=1}^4 a_i} \\ &= (-1)^\delta \frac{\Gamma(2+\delta)}{\prod_{j=1}^4 \Gamma(1+a_j)} \int_0^1 \prod_{k=1}^4 \Big[\mathrm{d}x_k\, x_k^{a_k}\Big]\, \delta\Big(1 - \sum_{i=1}^4 x_i\Big) \Big[x_1 x_3\, s + x_2 x_4\, t\Big]^{-2-\delta}. \end{aligned} \tag{3.13}$$

In order to evaluate the integral, we employ the Mellin–Barnes representation,[11] which yields

$$\begin{aligned} I_{\text{box}} &= \frac{1}{2\pi i} \frac{(-1)^\delta}{\prod_{j=1}^4 \Gamma(1+a_j)} \times \\ &\qquad \times \int_{-i\infty}^{i\infty} \mathrm{d}z \int_0^1 \prod_{k=1}^4 \Big[\mathrm{d}x_k\, x_k^{a_k}\Big]\, \delta\Big(1 - \sum_i x_i\Big) \frac{t^z}{s^{2+\delta+z}} \frac{(x_2 x_4)^z}{(x_1 x_3)^{z+2+\delta}} \Gamma(-z)\Gamma(z+2+\delta) \\ &= \frac{1}{2\pi i} \frac{(-1)^\delta}{\Gamma(-\delta)\prod_{j=1}^4 \Gamma(1+a_j)} \frac{1}{s^{2+\delta}} \times \\ &\qquad \times \int_{-i\infty}^{i\infty} \mathrm{d}z \left(\frac{t}{s}\right)^z \Gamma(1+a_2+z)\,\Gamma(1+\delta-a_1-a_2-a_3+z) \times \\ &\qquad\qquad \times \Gamma(a_1-1-\delta-z)\,\Gamma(a_3-1-\delta-z)\,\Gamma(2+\delta+z)\,\Gamma(-z), \end{aligned} \tag{3.14}$$

where the contour of integration is drawn in fig. 12. It separates the poles originating in the gamma functions with argument $\Gamma(\cdots - z)$ (right poles) from the poles of $\Gamma(\cdots + z)$ (left poles). In eq. (3.14) one can see why it was useful to keep the parameter δ explicit. Instead of being a regulator, it serves as an auxiliary variable in order to investigate the convergence of the integral. Yangian invariance requires $\delta = 0$; therefore one would naïvely conclude that the result is zero because of the prefactor $1/\Gamma(0)$. However, it is still possible for the integral to be nonvanishing if the integral diverges as $1/\delta$. We will investigate this issue.

[10] A curious fact is that no spinor quantities arise in the integral after Yangian invariance is imposed, when for general face variables they do. This suggests that the integral may be performed in dimensional regularisation, if required.

[11] We are grateful to Jan Plefka and Radu Roiban for discussions of this point.

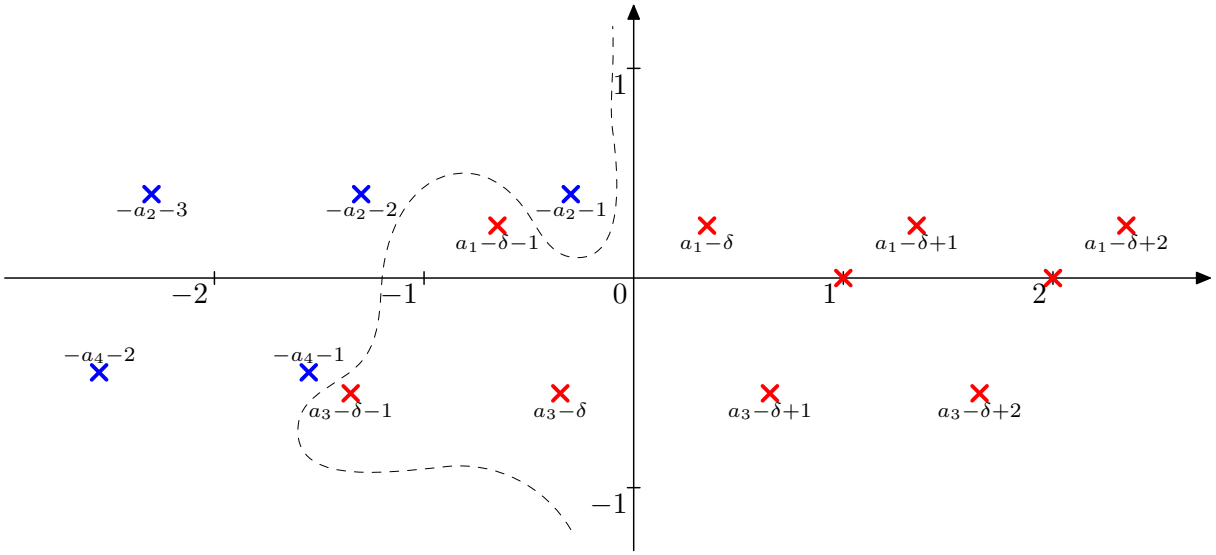

Figure 12: Poles in the MB representation of the amplitude. The dashed line is the integration contour.

The Mellin–Barnes integral diverges whenever a left and a right pole become coincident – a situation called *pinching* of poles. In order to extract the possibly divergent contribution, one has to split the contour of integration such that the right poles giving rise to the pinching are moved to the left. Accordingly, the contour integral splits into a convergent part arising from a new contour parallel to the imaginary axis and the residue integrals around the problematic right poles as drawn in fig. 13. Computing the two residues at $a_1 - 1 - \delta$ and $a_3 - 1 - \delta$ leads to

$$I_{\text{box}} = \frac{1}{s^{2+\delta}\Gamma(-\delta)} \left\{ \left(\frac{t}{s}\right)^{a_1-1-\delta} \frac{\Gamma(1+\delta-a_1)\Gamma(-\delta+a_1+a_2)\Gamma(-a_1+a_3)\Gamma(-a_2-a_3)}{\Gamma(1+a_2)\Gamma(1+a_3)\Gamma(1+\delta-a_1-a_2-a_3)} + \right.$$
$$\left. + \left(\frac{t}{s}\right)^{a_3-1-\delta} \frac{\Gamma(1+\delta-a_3)\Gamma(-\delta+a_2+a_3)\Gamma(a_1-a_3)\Gamma(-a_1-a_2)}{\Gamma(1+a_1)\Gamma(1+a_2)\Gamma(1+\delta-a_1-a_2-a_3)} \right\}. \tag{3.15}$$

Imposing $\delta = 0$ in eq. (3.15) clearly makes the integral vanish for generic values of a_1, a_2, a_3:

$$I_{\text{box}} = 0. \tag{3.16}$$

If this was the complete result, there would be a contradiction to the usual calculation of an undeformed four-point box integral. In particular, the undeformed box integral suffers from infrared divergences, whereas the above equality would imply it to vanish.

However, a more careful analysis shows that for specific values of a_1, a_2, a_3 the result may be nonzero. For example, when $a_1 + a_2 = 0$ and $a_2 + a_3 = 0$, the $1/\Gamma(-\delta)$ is cancelled in both terms of eq. (3.15). Hence, a double pole appears originating from two Γ's in the numerator. This suggests that the result is not identically zero, but rather a distribution with simultaneous support at $a_1 + a_2 = 0$ and $a_2 + a_3 = 0$. The derivation is subtle and requires much care. Using a heuristic derivation we find

$$I_{\text{box}}\Big|_{\delta=0} = -\delta(a_1+a_2)\,\delta(a_2+a_3)\,\frac{1}{s\,t}\left(\frac{t}{s}\right)^{a_1}\frac{\sin(a_1\pi)}{a_1}\,. \tag{3.17}$$

It is straightforward to check that this result is invariant under the exchange $s \leftrightarrow t$, provided that one exchanges also $a_1 \leftrightarrow a_4, a_2 \leftrightarrow a_3$, as can be deduced directly from the

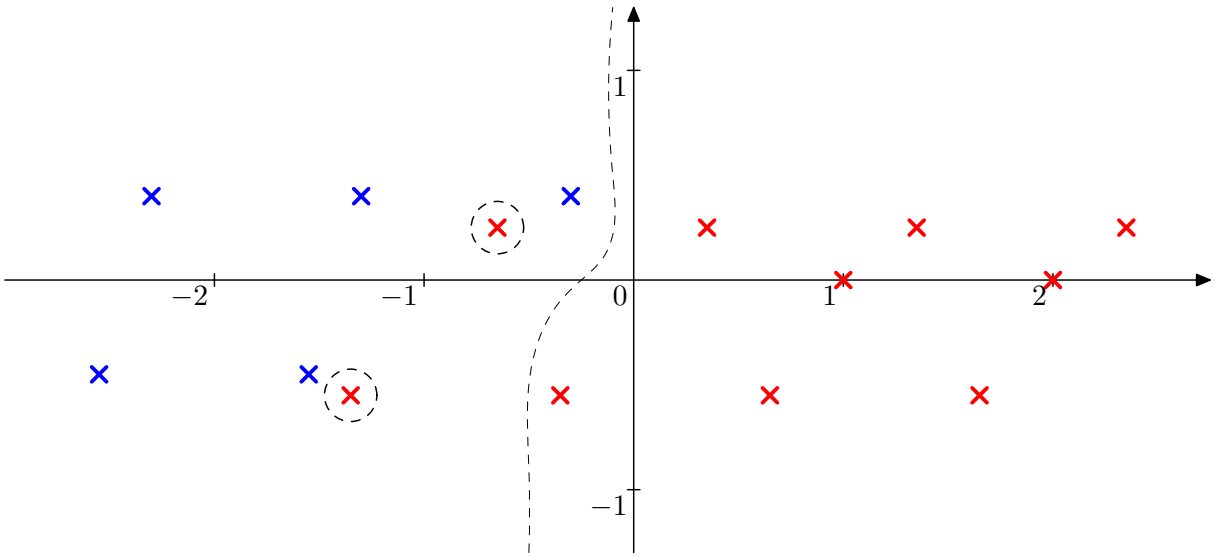

Figure 13: Contour of integration with possible pinchings disentangled; the two dashed circles represent residue integrals around the poles at $a_3 - \delta - 1$ and $a_1 - \delta - 1$, respectively.

integral of eq. (3.11). Moreover, the result in the undeformed case, $a_i = 0$, is proportional to $\delta^2(0)$ which could be argued to agree qualitatively with the $\log^2$ divergence of the undeformed integral. We refer to app. C for more details on our derivation.

3.5 Discussion

Let us briefly summarise our findings: In order to define deformed tree-level scattering amplitudes, there is only one object which can be deformed in a Yangian-invariant way without any further constraints: the top-cell. Integrating over the integrand corresponding to a deformed (tree-level) top-cell will lead to deformed MHV amplitudes.

Non-MHV tree-level amplitudes are built as a sum of Yangian invariant constituent graphs. While deforming each individual constituent graph works as for the top-cell, imposing compatibility between all graphs constrains the deformation parameters. While a few low-multiplicity examples still allow a deformation, the majority of non-MHV amplitudes cannot be deformed in this framework.

A possible way out would be the construction of Yangian-invariant scattering tree amplitudes in the non-MHV sector from constituent graphs which violate Yangian invariance individually, but sum up to an Yangian-invariant combination. It is not clear, whether this approach can be successful. Clearly, the formalism of deformed on-shell graphs explored in this paper is not applicable.

For what concerns amplitudes beyond tree-level, we restricted our study to the four-point one-loop case. In the undeformed case, this amplitude can be expressed via a single on-shell graph taking the rôle of the top-cell. The computation of the integral corresponding to the Yangian-invariant deformation of this on-shell graph yields a curious result: naïvely it would appear to be zero – which is trivially Yangian invariant. A more careful analysis suggests it to be a distribution with singular support.

For amplitudes of higher loop order and higher multiplicity, there is no known notion of an on-shell diagram comparable to the top-cell. Thus the situation is less clear than in the tree-level case.

4 Conclusions

In this paper, we describe a mechanism for constructing invariants of the Yangian algebra $\mathrm{Y}[\mathfrak{su}(2,2|4)]$ by combining trivalent invariant building blocks and maintaining invariance during the gluing procedure. The invariants are deformations of the on-shell diagrams put forward in ref. [6] which are invariants of $\mathrm{Y}[\mathfrak{psu}(2,2|4)]$. Deformation refers to a continuous shift of the central charges of the external legs introduced in [11].

The construction of deformed tree-level scattering amplitudes from deformed on-shell graphs works straightforwardly only for MHV amplitudes. With a few exceptions, the non-MHV amplitudes can not be deformed in the framework of (manifestly) Yangian-invariant on-shell graphs.

In ref. [15] it was argued that once one considers the holomorphic anomaly only, the complete S-matrix of $\mathcal{N}=4$ sYM is an invariant object as opposed to the constituent scattering amplitudes. For the deformed case we have argued that the interpretation of on-shell amplitudes as constituents of an S-matrix is all but evident. Nevertheless one could hope that the assumption of an exactly invariant composite object may lead the way to the identification of a suitable deformed S-matrix and its constituent on-shell graphs.

Finally, in ref. [11] it was suggested to employ the shifted helicities of the external legs as a regulator maintaining superconformal invariance. However, for the example of the one-loop amplitude, Yangian invariance was spoilt. If we stick with a Yangian-invariant deformation of the integrand, the resulting expression for the four-point one-loop amplitude will be zero for generic deformation parameters. For special deformations, however, the divergent behaviour of the integral is difficult to access. It depends on the particular way the deformation parameters are taken to zero.

Acknowledgements The authors would like to thank Claude Duhr, Livia Ferro, Tomasz Łukowski, Carlo Meneghelli, Jan Plefka, Matthias Staudacher, Cristian Vergu for discussions.

The work of NB and MR is partially supported by grant no. 200021-137616 from the Swiss National Science Foundation.

A Yangian invariance of deformed glued objects

In this appendix we provide the explicit calculation showing that an object obtained by gluing two deformed Yangian invariants is Yangian invariant if evaluation parameters and central charges are identified on the internal legs as in eq. (2.31). Let us consider two objects,

$$\mathcal{A}(1,\ldots,m,I),\ \mathcal{B}(I,m+1,\ldots,n)\ , \tag{A.1}$$

which are Yangian invariant, that is

$$\mathfrak{J}^a\cdot\mathcal{A}\ \equiv\ \Big[\sum_{i=1}^{I}\mathfrak{J}_i^a\Big]\cdot\mathcal{A}=0, \tag{A.2}$$

$$\widehat{\mathfrak{J}}^a\cdot\mathcal{A}\ \equiv\ \Big[f^a_{\ bc}\sum_{i=1}^{m}\sum_{j=i+1}^{I}\mathfrak{J}_i^b\,\mathfrak{J}_j^c+\sum_{k=1}^{I}u_k\,\mathfrak{J}_k^a\Big]\cdot\mathcal{A}=0\ , \tag{A.3}$$

and analogously for $\mathcal{B}$. Defining

$$\mathrm{d}^{4|4}\xi := \frac{\mathrm{d}^2\lambda_I\,\mathrm{d}^2\tilde{\lambda}_I}{\mathrm{Vol}[\mathrm{GL}(1)]}\,\mathrm{d}^{0|4}\eta_I\ , \tag{A.4}$$

the glued object reads

$$\mathcal{Y}(1,\ldots,n) = \int \mathrm{d}^{4|4}\xi\,\mathcal{A}(1,\ldots,m,I)\,\mathcal{B}(I,m+1,\ldots,n)\,. \tag{A.5}$$

It is invariant under the action of the level-zero generators for the same reason as in the undeformed case (see the discussion after eq. (2.15)), provided that it is annihilated by the total central charge operator $\mathfrak{C} = \sum_{i=1}^{n}\mathfrak{C}_i$. Combined with the Yangian invariance of $\mathcal{A}$ and $\mathcal{B}$, this implies that the central charges attached to the leg I of $\mathcal{A}$ must be the same (up to a sign) as the central charge attached to the leg I of $\mathcal{B}$.

In order to derive the condition for gluing the evaluation parameters, it is useful to note that the invariance of $\mathcal{Y}$ under the action of level-zero generators implies

$$\int \mathrm{d}^{4|4}\xi\,\Big[\big(\mathfrak{J}^a_I\mathcal{A}\big)\,\mathcal{B} + \mathcal{A}\,\big(\mathfrak{J}^a_I\mathcal{B}\big)\Big] \;=\; 0. \tag{A.6}$$

However, in order to fix the gluing condition for u_I, we have to consider the action of a level-one generator on the glued object:

$$\begin{aligned}
&\widehat{\mathfrak{J}}^a\cdot\int \mathrm{d}^{4|4}\xi\,\mathcal{A}(1,\ldots,m,I)\mathcal{B}(I,m+1,\ldots,n)\\
&=f^a_{bc}\int \mathrm{d}^{4|4}\xi\Big[\sum_{i=1}^{m}\sum_{j=i+1}^{m}\Big(\mathfrak{J}^b_i\mathfrak{J}^c_j\mathcal{A}\Big)\mathcal{B}+\sum_{i=1}^{m}\sum_{j=m+1}^{n}\Big(\mathfrak{J}^b_i\mathcal{A}\Big)\Big(\mathfrak{J}^c_j\mathcal{B}\Big)+\\
&\qquad\qquad+\sum_{i=m+1}^{n-1}\sum_{j=i+1}^{n}\mathcal{A}\Big(\mathfrak{J}^b_i\mathfrak{J}^c_j\mathcal{B}\Big)\Big]+\sum_{k=1}^{n}u_k\mathfrak{J}^a_k\int \mathrm{d}^{4|4}\xi\mathcal{A}\mathcal{B}\\
&=f^a_{bc}\int \mathrm{d}^{4|4}\xi\Big[\sum_{i=1}^{m}\sum_{j=i+1}^{I}\Big(\mathfrak{J}^b_i\mathfrak{J}^c_j\mathcal{A}\Big)\mathcal{B}-\sum_{i=1}^{m}\Big(\mathfrak{J}^b_i\mathfrak{J}^c_I\mathcal{A}\Big)\mathcal{B}+\sum_{i=1}^{m}\sum_{j=m+1}^{n}\Big(\mathfrak{J}^b_i\mathcal{A}\Big)\Big(\mathfrak{J}^c_j\mathcal{B}\Big)+\\
&\qquad\qquad-\sum_{j=m+1}^{n}\mathcal{A}\Big(\mathfrak{J}^b_I\mathfrak{J}^c_j\mathcal{B}\Big)+\sum_{i=m+1}^{n-1}\sum_{j=i+1}^{n}\mathcal{A}\Big(\mathfrak{J}^b_i\mathfrak{J}^c_j\mathcal{B}\Big)\Big]+\sum_{k=1}^{n}u_k\mathfrak{J}^a_k\int \mathrm{d}^{4|4}\xi\mathcal{A}\mathcal{B}
\end{aligned} \tag{A.7}$$

In the second and fourth term in the last line one can move the $\mathfrak{J}_I$ from $\mathcal{A}$ to $\mathcal{B}$ (paying a minus sign) and vice versa using (A.6). Then the second, third and fourth term can be combined into $(\mathfrak{J}^b\cdot\mathcal{A})(\mathfrak{J}^c\cdot\mathcal{B})$ which obviously vanishes. The remaining first and fifth term together with the term containing the evaluation parameters vanishes for all external legs leaving a contribution from the internal line I which reads

$$\widehat{\mathfrak{J}}^a\cdot\int\frac{\mathrm{d}^2\lambda\,\mathrm{d}^2\tilde{\lambda}}{\mathrm{Vol}[\mathrm{GL}(1)]}\,\mathrm{d}^{0|4}\eta_I\,\mathcal{A}\,\mathcal{B} = \int\frac{\mathrm{d}^2\lambda\,\mathrm{d}^2\tilde{\lambda}}{\mathrm{Vol}[\mathrm{GL}(1)]}\,\mathrm{d}^{0|4}\eta_I\Big[u_I^{\mathcal{A}}\Big(\mathfrak{J}^a_I\mathcal{A}\Big)\mathcal{B}+u_I^{\mathcal{B}}\mathcal{A}\Big(\mathfrak{J}^a_I\mathcal{B}\Big)\Big]\,. \tag{A.8}$$

Using the identity (A.6), one can show that the above expression vanishes if $u_I^{\mathcal{A}} = u_I^{\mathcal{B}}$. Therefore, superconformal and dual superconformal invariance imply that the evaluation parameters on internal legs match.

In a similar way, it is also possible to show that, given a Yangian invariant, the object obtained by identifying two adjacent legs and integrating over the on-shell superspace of that leg is again a Yangian invariant. Specifically, given an $(n+2)$-point Yangian invariant $\mathcal{Y}(1,\ldots,n+2)$, the object obtained via

$$\mathcal{Y}'(1,\ldots,n) = \int \frac{\mathrm{d}^2\lambda_I\,\mathrm{d}^2\tilde{\lambda}_I}{\mathrm{Vol}[\mathrm{GL}(1)]}\,\mathrm{d}^{0|4}\eta_I\,\mathcal{Y}(1,\ldots,n,I,J)|_{J=I} \tag{A.9}$$

is again Yangian invariant. The only nontrivial check is invariance under level-one generators; a sketch of the invariance (in the undeformed case) is as follows

$$\begin{aligned}
&\widehat{\mathfrak{J}}^a\cdot\int \mathrm{d}^{4|4}\xi\,\mathcal{Y}(1,\ldots,n,I,J)|_{I=J}\\
&=f^a_{\ bc}\int \mathrm{d}^{4|4}\xi\Big[\sum_{i=1}^{n-1}\sum_{j=i+1}^{n}\Big(\mathfrak{J}_i^b\mathfrak{J}_j^c\,\mathcal{Y}(1,\ldots,n,I,J)\Big)\Big]\Big|_{I=J}\\
&=-f^a_{\ bc}\int \mathrm{d}^{4|4}\xi\Big[\mathfrak{J}_I^b\mathfrak{J}_J^c\mathcal{Y}+\sum_{i=1}^{n}\Big(\mathfrak{J}_I^b\mathfrak{J}_I^c\mathcal{Y}\Big)+\sum_{i=1}^{n}\Big(\mathfrak{J}_I^b\mathfrak{J}_J^c\mathcal{Y}\Big)\Big]\Big|_{I=J}=\\
&=f^a_{\ bc}\int \mathrm{d}^{4|4}\xi\Big[\mathfrak{J}_I^b\mathfrak{J}_I^c\mathcal{Y}\Big]\Big|_{I=J}\propto f^a_{\ bc}f^{bc}_{\ d}\int \mathrm{d}^{4|4}\xi\,\Big[\mathfrak{J}_J^d\mathcal{Y}\Big]\Big|_{I=J}
\end{aligned} \tag{A.10}$$

which vanishes for $\mathfrak{psu}(2,2|4)$. In the derivation we implicitly used the invariance under the level-zero generators and the "integration-by-parts" identity

$$\int \mathrm{d}^{4|4}\xi\,\Big[\mathfrak{J}_I^a\mathcal{Y}(\ldots,I,J)+\mathfrak{J}_J^a\mathcal{Y}(\ldots,I,J)\Big]_{I=J}\;=\;0 \tag{A.11}$$

similar to eq. (A.6). The generalisation to the deformed case is straightforward and leads to the same conditions for c's and u's as before.

B Grassmannian integrals from on-shell graphs

One can associate a Grassmannian integral to any on-shell graph. The integral is most conveniently expressed in terms of the face variables f_i introduced in subsec. 3.1. As already stated there, the Grassmannian integral reads

$$\mathcal{I}_{\text{graph}}\;=\;\int\Big[\prod_{i=1}^{n_{\mathrm{F}}-1}\frac{\mathrm{d}f_i}{f_i}\Big]\,\delta^{2k}\Big(\sum_{a=1}^{n}C_{ra}(f_i)\tilde{\lambda}_a\Big)\,\delta^{2(n-k)}\Big(\sum_{s=1}^{n-k}C_{sa}(f_i)\lambda_a\Big)\,\delta^{0|4k}\Big(\sum_{a=1}^{n}C_{ra}(f_i)\tilde{\eta}_a\Big)\;, \tag{B.1}$$

where $C_{ra}(f_i)$ are elements of a $k\times n$ matrix that represents a point in $G(k,n)$. The expression of C_{ra} in terms of the face variables f_i is known (see ref. [6] for the precise construction).

What is more interesting from our point of view is that the integral can be expressed in terms of a different set of variables α which have a precise physical interpretation: they are related to the BCFW shift associated to adding a so-called BCFW bridge as depicted in fig. 14. The momentum flowing along the internal line is fixed to be proportional to $\lambda_i\tilde{\lambda}_j$ by the deltas of the two additional vertices while the external momenta are modified

$$\begin{aligned}
\lambda_{\hat{i}}\;&=\;\lambda_i, & \lambda_{\hat{j}}\;&=\;\lambda_j+\alpha\,\lambda_i,\\
\tilde{\lambda}_{\hat{i}}\;&=\;\tilde{\lambda}_i-\alpha\,\tilde{\lambda}_j, & \tilde{\lambda}_{\hat{j}}\;&=\;\tilde{\lambda}_j.
\end{aligned} \tag{B.2}$$

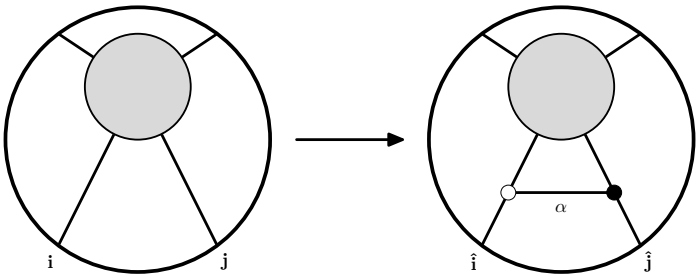

Figure 14: BCFW bridge construction

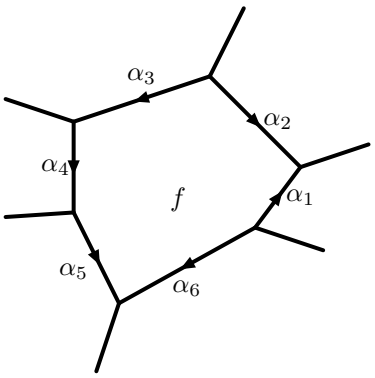

Figure 15: Face variable in terms of edge variables: here $f = \frac{\alpha_1\alpha_3\alpha_4\alpha_5}{\alpha_2\alpha_6}$

In ref. [6], it was demonstrated that the integral associated with an on-shell graph can be expressed in terms of these edge variables, the measure of integration being $\prod \frac{\mathrm{d}\alpha}{\alpha}$. Moreover, it is also possible to show that the removal of an edge I corresponds to taking the residue around $\alpha_I = 0$. Not all the edges of a graph are removable, but the ones that are can be identified from the permutation encoded by the graph.

It is possible to relate a face variable to the edge variables of the adjoining edges. In order to do so, one must introduce a specific orientation of the edges of the graph, called perfect orientation. Instead of describing the technicalities of perfect orientation, let us stick with the result: a face variable is given by the product of all the adjacent edge variables with counterclockwise orientation divided by the product of all the adjacent edge variables with clockwise orientation. An example is given in fig. 15.

Considering the removal of an edge in the deformed integral, it is evident that the measure in general will not be meromorphic in α. However, as pointed out in eq. (3.5), the deformed measure in terms of the face variables reads

$$\prod \frac{\mathrm{d}f_i}{f_i} \to \prod \frac{\mathrm{d}f_i}{f_i^{1+\zeta_i}}. \tag{B.3}$$

Focusing on one particular edge I, the related edge variable will appear in the measure as $\mathrm{d}\alpha_I/\alpha_I^{1+\zeta_i-\zeta_j}$, where i and j are the adjacent faces, since α_I appears in the numerator for one face variable and in the denominator for the other. The measure will be of the form $\frac{\mathrm{d}\alpha_I}{\alpha_I}$ if the difference of the face shifts of the two adjacent faces is zero: this is equivalent to no central charge flowing along the edge I.

C One-loop integral singular support

Here, we would like to argue that the deformed one-loop box integral eq. (3.11)

$$I_{\text{box}}(\{a_i\}; s, t) = \int \frac{\mathrm{d}^4 q}{(q^2)^{1+a_1}[(q+k_1)^2]^{1+a_2}[(q+k_1+k_2)^2]^{1+a_3}[(q-k_4)^2]^{1+a_4}} \tag{C.1}$$

in the form eq. (3.15) is expressed as a distribution with singular support, as in eq. (3.17).

Let us draw an analogy with the case of a single Dirac delta. One can define the Dirac delta function as the weak limit of the delta sequence

$$\eta_\epsilon(x) := \frac{1}{2\pi i}\left[\frac{1}{x-i\epsilon} - \frac{1}{x+i\epsilon}\right] = \frac{1}{\pi}\frac{\epsilon}{\epsilon^2+x^2}\,, \tag{C.2}$$

where η_ϵ satisfies the following limits:

$$\lim_{\epsilon\to 0} \eta_\epsilon(x) = 0 \qquad \text{for } x \neq 0, \tag{C.3}$$

$$\lim_{\epsilon\to 0} \epsilon\, \eta_\epsilon(c\epsilon) = \frac{1}{\pi(c^2+1)} \qquad \text{for } c \neq 0. \tag{C.4}$$

It is possible to show now that the function I_{box} defined in eq. (3.15) has a similar behaviour in the limit $\delta \to 0$. We already saw that the limit $\lim_{\delta\to 0} I_{\text{box}} = 0$ for generic a_1, a_2, a_3; we want now to probe the region where $a_1 \sim a_3 \sim (-a_2)$. We therefore consider I_{box} with $\sum_i a_i \propto \delta \neq 0$, study the region where

$$a_1 + a_2 \sim \delta\,, \qquad a_1 - a_3 \sim \delta\,, \tag{C.5}$$

and then take the limit $\delta \to 0$, in analogy with the limit taken in eq. (C.4).

Let us then rewrite the result of eq. (3.15) as a function of a_1, a_2, a_3, a_4, in order to obtain

$$\begin{aligned} I_{\text{box}} =& \frac{1}{s^{2+a_1+a_2+a_3+a_4}\Gamma(-a_1-a_2-a_3-a_4)}\times \\ &\times\left\{\left(\frac{t}{s}\right)^{-1-a_2-a_3-a_4}\frac{\Gamma(1+a_2+a_3+a_4)\Gamma(-a_3-a_4)\Gamma(-a_1+a_3)\Gamma(-a_2-a_3)}{\Gamma(1+a_2)\Gamma(1+a_3)\Gamma(1+a_4)}+\right. \\ &\left.+\left(\frac{t}{s}\right)^{-1-a_1-a_2-a_4}\frac{\Gamma(1+a_1+a_2+a_4)\Gamma(-a_1-a_4)\Gamma(a_1-a_3)\Gamma(-a_1-a_2)}{\Gamma(1+a_1)\Gamma(1+a_2)\Gamma(1+a_4)}\right\}. \end{aligned} \tag{C.6}$$

We subsequently set

$$a_1 = a + d_1\delta, \qquad a_2 = -a + d_2\delta, \qquad a_3 = a + d_3\delta, \qquad a_4 = -a + d_4\delta, \tag{C.7}$$

with $\sum_i a_i = d_{1234}\,\delta$,[12] where $d_{ij\ldots} := (d_i + d_j + \ldots)$. The limit we investigate is then

$$\lim_{\delta\to 0}\ \delta^2\, I_{\text{box}}\big(a + d_1\delta, -a + d_2\delta, a + d_3\delta, -a + d_4\delta\big). \tag{C.8}$$

We stress the logic we are trying to follow here. We saw that I_{box} is vanishing for generic configurations of a_i's, see eq. (3.16). We are now treating the parameter δ as the ϵ of the

[12] d_{1234} is just an overall scale for the d_i's; we can (and will) normalise them so that $d_{1234} = 1$.

delta sequence, eq. (C.3) and investigating the region where $a_1 + a_2 \sim \delta$, $a_1 - a_3 \sim \delta$, in analogy with the study of the delta sequence expressed in eq. (C.4) in the region $x \sim \epsilon$.

The result of the limit in eq. (C.8) is

$$\begin{aligned}\lim_{\delta\to 0}\ \delta^2 I &= -\frac{1}{s\,t}\frac{(t/s)^a}{\Gamma(1+a)\Gamma(1-a)}\frac{(d_{1234})^2}{d_{12}\,d_{23}\,d_{34}\,d_{41}} \\ &= -\frac{1}{s\,t}\frac{(t/s)^a}{\Gamma(1+a)\Gamma(1-a)}\left[\frac{1}{d_{12}\,d_{23}}+\frac{1}{d_{23}\,d_{34}}+\frac{1}{d_{34}\,d_{41}}+\frac{1}{d_{41}\,d_{12}}\right].\end{aligned} \tag{C.9}$$

We can always rescale δ, so we set $d_{1234} = 1$. This leads to

$$\lim_{\delta\to 0}\ \delta^2 I_{\rm box} = \frac{1}{s\,t}\frac{(\frac{t}{s})^a}{\Gamma(1-a)\Gamma(1+a)}\frac{1}{(d_{12}-1)(d_{12})(d_{23}-1)(d_{23})}, \tag{C.10}$$

a result which is similar to eq. (C.4), but not equal; however, the explicit form of the limit should depend on the direction along which the limit of all a_i's to be equal (up to a sign) is taken. It is possible to get an expression with the same residues as eq. (C.4) if we shift the a_i's differently, as

$$\lim_{\delta\to 0}\ \delta^2\, I_{\rm box}\Big(a + d_1\delta,\ -a + \big(d_2 + \tfrac{i}{2}\big)\delta,\ a + d_3\delta,\ -a + \big(d_4 - \tfrac{i}{2}\big)\delta\Big) := \lim_{\delta\to 0}\ \delta^2\, I'_{\rm box}, \tag{C.11}$$

where we have defined a different shift for a_2 and a_4, keeping fixed the condition $\sum_i a_i = d_{1234}\,\delta$. The above equation leads to

$$\lim_{\delta\to 0}\ \delta^2\, I'_{\rm box} = -\frac{1}{s\,t}\left(\frac{t}{s}\right)^a \frac{16\sin(a\pi)}{a\pi}\frac{1}{(4d_{12}^2+1)(4d_{23}^2+1)} \tag{C.12}$$

which, considering also eq. (C.4) (with $c \to c/2$), leads to (cf. eq. (3.17))

$$I_{\rm box} = -\delta(a_1+a_2)\,\delta(a_2+a_3)\,\frac{1}{s\,t}\left(\frac{t}{s}\right)^{a_1}\frac{\sin(a_1\pi)}{a_1}. \tag{C.13}$$

There are however two remarks to be stressed. The first is that the choice of shift in eq. (C.11) leads to a nonvanishing result with a clear interpretation, but is *ad hoc*. The second is the argument leading to eq. (C.13) is rather heuristic, based on the fact that the behaviour of $I_{\rm box}$ in the limit $\delta \to 0$ (and for a particular choice of direction along with the a_i's approach zero) is similar to the behaviour of a delta sequence.

References

[1] J. M. Drummond, J. M. Henn and J. Plefka, *"Yangian symmetry of scattering amplitudes in N=4 super Yang-Mills theory"*, JHEP 0905, 046 (2009), arxiv:0902.2987.

[2] R. Roiban, M. Spradlin and A. Volovich, (eds.), *"Scattering Amplitudes in Gauge Theories: Progress and Outlook"*, J. Phys. A 44, 450301 (2011).

[3] N. Beisert, *"On Yangian Symmetry in Planar N=4 SYM"*, arxiv:1004.5423.

[4] J. M. Drummond, J. Henn, G. P. Korchemsky and E. Sokatchev, *"Dual superconformal symmetry of scattering amplitudes in N=4 super-Yang-Mills theory"*, Nucl. Phys. B828, 317 (2010), arxiv:0807.1095.

[5] N. Beisert et al., *"Review of AdS/CFT Integrability: An Overview"*, Lett. Math. Phys. 99, 3 (2012), arxiv:1012.3982.

[6] N. Arkani-Hamed, J. L. Bourjaily, F. Cachazo, A. B. Goncharov, A. Postnikov and J. Trnka, *"Scattering Amplitudes and the Positive Grassmannian"*, arxiv:1212.5605.

[7] N. Arkani-Hamed, F. Cachazo, C. Cheung and J. Kaplan, *"A Duality For The S Matrix"*, JHEP 1003, 020 (2010), arxiv:0907.5418.

[8] J. M. Drummond and L. Ferro, *"Yangians, Grassmannians and T-duality"*, JHEP 1007, 027 (2010), arxiv:1001.3348. • J. M. Drummond and L. Ferro, *"The Yangian origin of the Grassmannian integral"*, JHEP 1012, 010 (2010), arxiv:1002.4622.

[9] N. Arkani-Hamed, J. L. Bourjaily, F. Cachazo, S. Caron-Huot and J. Trnka, *"The All-Loop Integrand For Scattering Amplitudes in Planar N=4 SYM"*, JHEP 1101, 041 (2011), arxiv:1008.2958.

[10] N. Arkani-Hamed, J. L. Bourjaily, F. Cachazo and J. Trnka, *"Local Integrals for Planar Scattering Amplitudes"*, JHEP 1206, 125 (2012), arxiv:1012.6032.

[11] L. Ferro, T. Łukowski, C. Meneghelli, J. Plefka and M. Staudacher, *"Harmonic R-matrices for Scattering Amplitudes and Spectral Regularization"*, Phys. Rev. Lett. 110, 121602 (2013), arxiv:1212.0850. • L. Ferro, T. ukowski, C. Meneghelli, J. Plefka and M. Staudacher, *"Spectral Parameters for Scattering Amplitudes in N=4 Super Yang-Mills Theory"*, JHEP 1401, 094 (2014), arxiv:1308.3494.

[12] R. Britto, F. Cachazo and B. Feng, *"New recursion relations for tree amplitudes of gluons"*, Nucl. Phys. B715, 499 (2005), hep-th/0412308. • R. Britto, F. Cachazo, B. Feng and E. Witten, *"Direct proof of tree-level recursion relation in Yang-Mills theory"*, Phys. Rev. Lett. 94, 181602 (2005), hep-th/0501052. • N. Arkani-Hamed, F. Cachazo and J. Kaplan, *"What is the Simplest Quantum Field Theory?"*, JHEP 1009, 016 (2010), arxiv:0808.1446. • A. Brandhuber, P. Heslop and G. Travaglini, *"A Note on dual superconformal symmetry of the N=4 super Yang-Mills S-matrix"*, Phys. Rev. D78, 125005 (2008), arxiv:0807.4097.

[13] L. J. Mason and N. M. J. Woodhouse, *"Integrability, selfduality, and twistor theory"*, Oxford University Press, Oxford, UK (1991).

[14] E. Witten, *"Perturbative gauge theory as a string theory in twistor space"*, Commun. Math. Phys. 252, 189 (2004), hep-th/0312171.

[15] T. Bargheer, N. Beisert, W. Galleas, F. Loebbert and T. McLoughlin, *"Exacting N=4 Superconformal Symmetry"*, JHEP 0911, 056 (2009), arxiv:0905.3738.

[16] T. Bargheer, N. Beisert and F. Loebbert, *"Exact Superconformal and Yangian Symmetry of Scattering Amplitudes"*, J. Phys. A44, 454012 (2011), arxiv:1104.0700.

[17] T. Bargheer, N. Beisert, F. Loebbert and T. McLoughlin, *"Conformal Anomaly for Amplitudes in N=6 Superconformal Chern-Simons Theory"*, J. Phys. A45, 475402 (2012), arxiv:1204.4406.

[18] S. Caron-Huot, *"Loops and trees"*, JHEP 1105, 080 (2011), arxiv:1007.3224.

[19] Z. Bern, L. Dixon, D. Kosower, R. Roiban, M. Spradlin et al., *"The Two-Loop Six-Gluon MHV Amplitude in Maximally Supersymmetric Yang-Mills Theory"*, Phys. Rev. D78, 045007 (2008), arxiv:0803.1465.

[20] A. Postnikov, *"Total positivity, Grassmannians, and networks"*, math/0609764.